The microenvironment resulting from the co-culture of human amniotic fluid-derived mesenchymal stem cells with peripheral blood mononuclear cells differs between type 1 diabetes mellitus patients and healthy individuals

Seyed Mehdi Hoseini
https://orcid.org/0000-0001-8759-2712
Farnoosh Moghimi
Elham Sadat Hosseini
Seyed Mohsen Miresmaeili
Mohammad Yahya Vahidi Mehrjardi
Mohammad Reza Dehghani
Mohammad Hasan Sheikhha
Fateme Montazeri (f_montazeri@Outlook.com)
https://orcid.org/0000-0002-1984-951X

Research Article

Keywords: Cell contact, Chemokines, Mesenchymal stem cells, Paracrine factor, Type 1 diabetes mellitus

Posted Date: September 21st, 2023

DOI: https://doi.org/10.21203/rs.3.rs-3311428/v2

Abstract

IFNγ is one of the main factors involved in type 1 diabetes (T1D) pathogenesis and has also been used to license mesenchymal stem cells (MSCs) for displaying immunosuppressive properties in a process termed preconditioning/priming. Our study aimed to investigate the interaction of amniotic fluid-derived MSCs (AF-MSCs) in two preconditioned (IFNγ) and non-preconditioned (IFNγ) conditions, with peripheral blood mononuclear cells (PBMCs) from the sources of healthy control (HC) and T1D. Accordingly, the interactions were assessed through anti-inflammatory genes, chemokines and their receptors, plus the induction of T regulatory (Treg) cells. Our results demonstrated that MSC/IFNγ and MSC/IFNγ treatments respond conversely to HC and T1D PBMCs regarding the expression of anti-inflammatory genes (*IDO1*, *IDO2*, *ICAM-1*), chemokine ligands (*CCL3*, *CXCL9, CXCL10*) and receptors involved in immune cell trafficking (*CXCR3*, *CXCR6*, *TLR4*). Our findings also confirmed the same opposite effects of HC and T1D PBMCs when interacting with IFNγ and IFNγ MSCs regarding the expression of target genes, including *CXCR3* and its ligands (*CXCL9* and *CXCL10*), *CXCR6*, *CCR5* and its ligands (*CCL3* and *CCL4*). These differences were also reflected in the proportion of Treg cells in HC and T1D samples, depending on whether it was assessed through paracrine or cell contact approaches. Our research indicates that the interaction between IFNγ and IFNγ MSCs and T1D PBMCs creates distinct microenvironments compared to those in HC PBMCs. This implies that the intravenous administration of MSCs into T1D patients may result in different outcomes than in healthy individuals that can be manipulated by the preconditioning of MSCs.

Introduction

Autoimmune destruction of insulin-producing β-cells in the pancreatic islets causes an inflammatory reaction called insulitis which leads to Type 1 diabetes mellitus (T1DM) usually in children and young adults (Figliuzzi et al. 2014). Indeed, T1D arises due to the disruption of the homeostatic balance between regulatory T (Treg) cells and T helper-1 (Th1) cells, including CD4 and CD8 , as well as other IFNγ-producing cells (Sandor, Jacobelli, and Friedman 2019). The lack of effective therapeutics blocking the recruitment of MNPs and lymphocytes toward the islets arises from our incomplete understanding of their chemotaxis in the microenvironment of inflamed tissues (Sandor et al. 2019). The targeted destruction of specific parenchymal tissues is related to the localization of motile immune cells and their spatiotemporal regulation. Therefore, the pathogenesis of T1D depends on the factors controlling immune cell trafficking and their bioactivity that can be potentially considered as the therapeutic target for the treatment of such autoimmune diseases (Sarkar et al. 2012). In this regard, chemokines and their cognate receptors perform an indispensable function in the recruitment and chemotaxis of immune cells to the site of inflammation. Hence, these molecules have emerged as potential biomarkers and therapeutic targets in numerous autoimmune disorders, including T1D (Griffith, Sokol, and Luster 2014; Sarkar et al. 2012).

Over the last decade, mesenchymal stem/stromal cells (MSCs) have been introduced as a promising strategy for the treatment of broad autoimmune diseases including T1D (Yang et al. 2021; Figliuzzi et al.

2014). These cells with self-renewal and multiple differentiation characteristics can be isolated from adult tissues (e.g., bone marrow, adipose, and dental pulp tissues) as well as perinatal sources (e.g., umbilical cord blood, placenta, amniotic fluid) (Yang et al. 2021; Hoseini, Kalantar, et al. 2020; Hoseini et al. 2021; Hoseini, Montazeri, Bahrami, et al. 2020). However, the cell therapy approach requires a precise understanding of the behavior of MSCs in the microenvironment of inflamed pancreatic islets in T1D patients. The microenvironment of MSCs is the most important factor in determining their regulatory effects on the immune cells. The plasticity of MSCs plays a key role in their immunoregulatory characteristics, meaning that based on the environmental stimuli these cells exert both pro-inflammatory and anti-inflammatory influence on the immune system (Bernardo and Fibbe 2013; Hoseini, Montazeri, Kalantar, et al. 2020). MSCs regulate tissue homeostasis and integrity by adopting these contradictory phenotypes through interaction with both innate and adaptive immune cells. For this purpose, MSCs become polarized and express different markers and mediators that prepare them for their anti- or pro-inflammatory roles (Le Blanc and Davies 2015).

The pro-inflammatory cytokines, particularly IFNγ and TNFα, are the most important factors to polarize MSCs and switch them from an unlicensed to an activated state (Bernardo and Fibbe 2013). Moreover, IFN-γ-enriched microenvironment around inflamed islets can drive the expression of IFN-stimulated genes, including chemokines and their receptors (Calderon et al. 2011; Sarkar et al. 2012; Fallahi et al. 2016; Burke and Collier 2015). Therefore, the local milieu at the site of inflammation is decisive for inducing the functional activity of MSCs (Zhou et al. 2019; Suzdaltseva et al. 2022). Studies on the tumor microenvironment (TME) have shown that tumor-associated chronic inflammation provides signals in the inflamed microenvironment to license MSCs to exert their immunosuppressive phenotype in favor of tumor progression (Trivanović et al. 2016). The release of MSCs from the bone marrow into the peripheral blood and homing to the inflamed islets, plus tissue-resident MSCs may play a prominent same role in the islets microenvironment (Han et al. 2012; Yin et al. 2018; Hu et al. 2003). Previous studies confirm the role of IFNγ to create an inflammatory microenvironment in the islets and consequently upregulating adhesion molecules and chemokines there. However, the effect of IFNγ on other components of the islet microenvironment, especially on tissue-resident MSCs, remains unclear. Accordingly, this study hypothesized that the bidirectional interactions between PBMCs and MSCs could be affected by the function of IFNγ as well as paracrine and cell contact effects in terms of the expression of chemokines and their receptors, as well as induction of Treg cells.

Materials And Methods

2.1. Sampling under ethics guidelines

Based on the hypothesis of the study about the differential response of immune cells from healthy individuals and T1D patients, to MSCs, peripheral blood mononuclear cells (PBMCs) were isolated from two sources, i.e., healthy control (HC) and new-onset T1D patients, while MSCs were derived from a single source. For this purpose, 15 ml of heparinized whole blood was collected from three male volunteers newly diagnosed with T1D (referred to Yazd Diabetes Research Center, Shahid Sadoughi

University of Medical Sciences) and three healthy donors, all six men ranged from 20 to 25 years old. To derivation of MSCs, 20 ml of amniotic fluid was collected through the procedure of amniocentesis (for prenatal diagnosis-PND) from a healthy pregnant woman carrying a male fetus at 16 weeks gestational age. All volunteers have signed the informed consent form according to the guidelines of the Ethics Committee of Shahid Sadoughi University of Medical Sciences.

2.2. Human peripheral blood mononuclear cells

The peripheral blood of volunteers was obtained by heparinized syringe and then PBMCs were purified using density gradient centrifugation through Lymphocyte Separation Solution (from Serana) based on the manufacturer's manual. The cell pellet of PBMCs was twice washed with Hanks' Balanced Salt Solution (HBSS) and medium RPMI-1640, respectively, and centrifugation cell suspension in 400 *g* for 10 min. The freshly isolated PBMCs were cultured in T25 flasks at 37°C and under 5% humidified CO_2 for 48 h using RPMI-1640 supplemented with 15% fetal bovine serum (FBS), 1% Penicillin-Streptomycin (Pen-Strep) and 5 µg/ml phytohemagglutinin A (PHA) as a mitogenic lectin known for its ability to stimulate PBMC proliferation. All ingredients and additives were from Gibco, including RPMI-1640, FBS, Pen-Strep, and PHA.

2.3. Human amniotic fluid-derived mesenchymal stem cells

The supernatant of the primary culture of amniocytes discarded routinely during the prenatal diagnosis (PND) process was used to derive MSCs from amniotic fluid (AF-MSCs). The primary cultures contained AmnioMAX-II complete medium supplemented with 20 mM HEPES, 1% Pen-Strep (all from Gibco), and incubated at 37°C in a dry incubator without CO_2. To derive MSCs, the supernatant of primary cultures was centrifuged at 400 *g* for 15 min, and then the cell pellet was cultured in a 6-well plate by DMEM-AmnioMAX-II (2:1 v/v) modified medium at 37°C and under 5% humidified CO_2. DMEM with 4 mM L-Glu (from Gibco) was supplemented by 10 mM HEPES, 15% FBS, and 1% Pen-Strep. The proper clones from each well were expanded during long-term cultivation in T25 flasks in the same condition. The cell expansion lasted until the third passage when the cells were harvested for flow cytometry analysis and prepared for co-culture experiments. For the latter aim, derived AF-MSCs were seeded at a density of 10^4 cells/cm^2 into 6-well plates (nearly 10^5 cells/well) in basal medium (DMEM with 10% FBS) and cultured for 48 h in two different conditions, including basal state without stimulation and IFN-γ stimulated state by 100 international units (IU)/ml of basal medium. The supernatant of these cultures was finally collected to be used in intended experiments as the conditioned medium of MSCs (MSC-CM). Additionally, the drained 6-well plates (with almost 80% confluency) became refreshed by the same volume of basal medium to be used in co-culture experiments.

2.4. Mesodermal differentiation of mesenchymal stem cells

The differentiation capacity of AF-MSCs was examined for adipogenesis and osteogenesis. The cells in the third passage were seeded in 6-well plates at a density of 5×10^3 cells/cm^2

by basal medium, DMEM containing 10% FBS and 1% Pen-Strep. Following 70% confluency, the cultures were refreshed by differentiation medium for 3 weeks (refreshing medium every 3 days). The adipogenic medium was composed of basal medium supplemented by 50 µg/ml indomethacin, 50 µg/ml ascorbic acid-2-phosphate, and 100 nM dexamethasone. Also, for osteogenic differentiation, the basal medium was supplemented by 10 mM β-glycerol phosphate, 50 µg/ml ascorbic acid-2-phosphate, and 10 nM dexamethasone (all supplements were from Sigma-Aldrich). To confirm adipogenesis in the cells, intracellular lipid vacuoles were stained with the Oil Red O (Sigma Aldrich). Validation of osteogenesis can be visualized via staining of extracellular matrix mineralization by Alizarin Red (Kornicka et al. 2015).

2.5. Co-culture and conditioned medium experiments

The experiments in the study were designed in two parts; PBMCs co-cultured with MSCs and PBMCs cultured with MSC-CM, both in four different treatments (a total of 8 treatments). Accordingly, four different treatments were designed through co-cultures to evaluate the direct interaction of MSCs and PBMCs, so that two sources of PBMCs (from T1D and healthy control) co-cultured with differently preconditioned MSCs (non-stimulated and IFNγ-stimulated) at a concentration of 0.5×10^6 cells/ml of basal medium. Similarly, two sources of PBMCs were also cultured at the same concentration (0.5×10^6 cells/ml) of MSC-CM collected from differently preconditioned cultures. Furthermore, two sources of PBMCs were also cultivated alone as the basic culture at the concentration of 0.5×10^6 cells/ml of basal medium. Altogether, a total of 10 treatments in triplicate samples, were incubated in humidified atmosphere at 37°C and 5% CO_2 for 72 h.

2.6. Flow cytometry analysis

In this study, the flow cytometry analysis was used for two purposes: 1) characterization of MSCs at the third passage based on the common mesenchymal markers, including CD73, CD90, and CD105 as positive markers and CD34 as negative ones; 2) evaluation of T regulatory (Treg) cells in different treatments of PBMCs via Treg-specific conjugates, including CD4, CD25, and Foxp3. For the former purpose, at least 1×10^5 cells for each assay were detached from T25 flasks by trypsin-EDTA treatment, and the collected cell pellet was washed twice in phosphate-buffered saline (PBS) containing 0.2% FBS. Cells were then incubated with the pertaining antibodies in a solution of PBS supplemented with 1% bovine serum albumin (BSA), including CY7-conjugated anti-human CD73, APC-conjugated anti-human CD90, PE-conjugated anti-human CD105, and FITC-conjugated anti-human CD34. The conjugates were from Immunostep and Exbio. For the latter purpose, PBMCs were collected from 3 samples of each treatment (5 from each HC and T1D cell source) and pooled as 10 mimetic situations to analyze Treg cells in 10 treatments. The PBMCs were centrifuged from co-cultures, MSC-CM, and basic cultures, then washed twice with PBS containing 0.2% FBS and similarly treated for incubation of Treg-specific conjugates. The PBMCs were gated three times by the cell size of lymphocytes, $CD4^+$ lymphocytes, and among these, $CD25^+$, and $Foxp3^+$ cells. The results were analyzed on a BD FACSCalibur and the graphs were generated in FlowJo (v 10.1, Tree Star, Inc.) software.

2.7. Molecular analysis

The technique of reverse transcription-polymerase chain reaction (RT-PCR) was used for quantitative analysis of intended genes in the interaction of MSCs and PBMCs. Accordingly, total RNA was extracted from the cells by TRIzol reagent (Roche). Following qualitative and quantitative assessment of isolated RNA, 100 ng of total RNA was used to synthesize cDNA via the RevertAid First Strand cDNA Synthesis Kit (Thermo Scientific). Applied Biosystems® SYBR® Green PCR Master Mix was used for the preparation of RT-PCR reactions which was carried out using Applied Biosystems StepOnePlus Real-Time PCR System. The thermal profile of these reactions was set on the initial denaturation step at 95°C for 10 min, then 40 cycles of 95°C for 15 secs, 58-60°C (based on different Tm of primers) for 20 secs, and 72°C for 30 secs.

The intended genes for investigating the immunomodulatory properties of AF-MSCs co-cultured with PBMCs were *indoleamine 2,3-dioxygenase 1* and *2* (*IDO1* and *IDO2*). Moreover, cell contact is also an essential mechanism in immunomodulatory, so AF-MSCs were examined for *intercellular adhesion molecule-1* (*ICAM-1*), and a range of genes involved in chemokine/receptor interactions, including the receptors of *C-X-C motif chemokine receptor 3* and *6* (*CXCR3* and *CXCR6*, respectively), as well as the ligands of *C-C motif chemokine ligand 3* (*CCL3*), *C-X-C motif chemokine ligand 9* and *10* (*CXCL9* and *CXCL10*, respectively). As responsible for pro-inflammatory immune responses, *toll-like receptor 4* (*TLR4*) was measured in both AF-MSCs and PBMCs. For immune cell trafficking, PBMCs were also assessed for nearly the same ligand and receptor genes, including the chemokine ligands *CCL3*, *CCL4*, *CXCL9,* and *CXCL10* as well as the receptors *CXCR3*, *CXCR6*, and *C-C motif chemokine receptor 5* (*CCR5*). *18S rRNA* was used as a reference gene in all RT-PCR reactions. All primers are designed for human-specific, intron-spanning targets and their sequences and the size of amplified products are listed in Table 1.

2.8. Statistical analysis

The quantitative assessment of RT-PCR results was performed by $2^{\Delta CT}$ methods in which the difference between reference and target C_T values of each sample was taken into account for analysis. The average expression levels for each gene were analyzed by non-parametric *t*-test and analysis of variance (ANOVA) at the significant level of *p*-value < 0.05. The Pearson correlation analysis was also used to determine the possible correlations of target genes with each other among individual treatments. Accordingly, Pearson's coefficient ranged from "-1" to "1", but only values of "0.9 to 1" (positive correlations) and "-0.9 to -1" (negative correlations) with *p*-values < 0.05 were significantly correlated.

Results

3.1. Isolation of PBMCs, derivation of AF-MSCs and their co-culture

Freshly isolated PBMCs from 3 unrelated healthy and 3 T1D donors were cultured for 48 h to be activated by PHA. The cultivated PBMCs which are depicted in Fig.1-A as an example were evaluated following the activation course. Using trypan blue exclusion (staining dead cells), viable PBMCs were analyzed by

counting a series of dilutions manually. The results confirmed significantly higher cell concentration in the healthy control (HC) than in the T1D group (*p*-value < 0.05) (Fig.1-B). The derived AF-MSCs which were expanded until the third passage (when characterized as MSCs) are illustrated in Fig.1-C. Similarly, these cells were also cultured for 48 h to be attached to the intended plates of experiments and/or to be stimulated by IFN-γ as a preconditioning phase (if needed based on the experimental design).

3.2. Characterization of amniotic fluid-derived mesenchymal stem cells

Based on the International Society for Cellular Therapy (ISCT) minimal criteria for classifying clonal cells as MSCs, adherent cells express the surface antigens of CD73, CD90, and CD105, as well as lacking expression of hematopoietic markers such as CD34. In our study, the expanded cells until the third passage were characterized by flow cytometry to examine the percentage of cells expressing the positive and negative markers of intended. Firstly, to confirm the non-hematopoietic origin of expanded cells, CD34 was investigated as a negative marker and the results demonstrated that more than 99% of the cells were negative for CD34 (Fig.2-A). The results of flow cytometry analysis also revealed a homogeneous cell population in which more than 98% of the cells positively expressed the desired MSC markers, including CD73, CD90, and CD105, as illustrated in Fig.2-B, -C, and -D, respectively. Moreover, the mesodermal differentiation ability of our cells into adipocytes and osteocytes was examined to verify the cells as AF-MSCs. Our results confirmed the capacity of AF-MSCs to differentiate into adipocytes and osteocytes, which are illustrated in Fig. 2-E and -F, respectively.

3.3. Molecular analysis of AF-MSCs

AF-MSCs were analyzed in 4 treatments, preconditioned with IFNγ (IFNγ) and non-preconditioned (IFNγ) that were then co-cultured with HC and T1D PBMCs. Accordingly, these MSCs were assessed for 9 genes of interest at the end of co-culture experiments, including the anti-inflammatory agents *IDO1*, *IDO2*, and *ICAM-1*, the chemokine ligands *CCL3*, *CXCL9,* and *CXCL10*, as well as the receptors involved in immune cell trafficking, *CXCR3*, *CXCR6*, and *TLR4*.

3.3.1. Quantitative expression of anti-inflammatory agents in AF-MSCs

The relative expression of anti-inflammatory genes was evaluated in AF-MSCs after the co-culture treatments. As illustrated in Fig.3-A, -B, and -C, *IDO1*, *IDO2*, and *ICAM-1* (respectively) were expressed in a similar trend among treatments, though *IDO2* by higher levels (based on the Y-axis scale). The results showed that IFNγ cells expressed these genes at higher levels when they were co-cultured with T1D PBMCs compared to HC PBMCs, however, the increase of *IDO1* and *ICAM-1* was significant (*p*-value = 0.020 and 0.046, respectively) but non-significant in *IDO2* (*p*-value = 0.463). On the contrary, the genes were substantially upregulated in IFNγ cells following the co-culture with HC PBMCs than that with T1D PBMCs, significantly for *IDO1* and *ICAM-1* (*p*-value = 0.010 and 0.001, respectively) and insignificantly for *IDO2* (*p*-value = 0.189). Furthermore, the mixed model of the ANOVA test revealed a significant interaction of treatments on each other regarding the *IDO1* (*p*-value = 0.0005), so that MSC/IFNγ and MSC/IFNγ responded conversely in interaction with different sources

of PBMCs (fig.3-A). The same analysis on the *ICAM-1* expression indicated that the preconditioning strategy caused a substantial downregulation in MSC/IFNγ (*p*-value = 0.0002), particularly in co-culture with HC PBMCs.

3.3.2. Quantitative expression of chemokine ligands in AF-MSCs

The relative expression of chemokine ligands, *CCL3*, *CXCL9,* and *CXCL10*, were evaluated in AF-MSCs at the end of co-culture experiments. As illustrated in fig.3-D, *CCL3* was increased in both preconditioned and non-preconditioned AF-MSCs during the co-culture with HC PBMCs compared to the T1D PBMCs, significantly by MSC/IFNγ (*p*-value = 0.014) and insignificantly by MSC/IFNγ (*p*-value = 0.411). Although the difference between MSC/IFNγ and MSC/IFNγ was non-significant (*p*-value = 0.064), there was a noticeable interaction among treatments (*p*-value = 0.017). Accordingly, IFNγ cells co-cultured with HC PBMCs exhibited a high level of *CCL3*, whereas they barely expressed it during the co-culture with T1D PBMCs. It seems that the preconditioning process is responsible for this substantial change and plays a role in this regard. Therefore, a milder difference was observed in the treatments of IFNγ cells, meaning that compared to IFNγ cells, MSC/IFNγ considerably declined the level of *CCL3* after co-culture with HC PBMCs while conversely raised it during the co-culture with T1D PBMCs.

As illustrated in Fig.3-E and -F, *CXCL9,* and *CXCL10* were insignificantly changed in MSC/IFNγ in response to the co-culture with two sources of PBMCs (*p*-value = 0.381 and *p*-value = 0.749, respectively). Contrariwise, these genes were significantly modified in MSC/IFNγ due to the interaction with different PBMCs. However, the IFNγ cells displayed an inverse expression pattern among the treatments, so they upregulated *CXCL9* during the co-culture with T1D PBMCs (*p*-value = 0.011) but increased *CXCL10* in interaction with HC PBMCs (*p*-value = 0.012). Despite the differences, the results of the ANOVA test demonstrated that both genes were similarly downregulated by the two treatments of IFNγ cells (*p*-value = 0.006 for *CXCL9* and *p*-value = 0.0005 for *CXCL10*).

3.3.3. Quantitative expression of receptors about cell trafficking in AF-MSCs

The target genes involved in immune cell trafficking, *CXCR3*, *CXCR6*, and *TLR4*, were evaluated in AF-MSCs at the end of co-culture experiments. As illustrated in Fig.3-G and -H, the chemokine receptors *CXCR3* and *CXCR6* (respectively) demonstrated an inverse expression pattern among the treatments. The IFNγ cells insignificantly downregulated *CXCR3* (*p*-value = 0.322), but significantly upregulated *CXCR6* (*p*-value = 0.018) when they were co-cultured with T1D PBMCs in comparison with the HC PBMCs. Nonetheless, the IFNγ cells responded to the co-culture experiments in a reverse way. Although these experiments revealed non-significant results concerning the levels of both genes in MSC/IFNγ , the ANOVA test calculated a significant interaction between the expression levels of *CXCR6* among 4 co-culture treatments (*p*-value = 0.005). The expression of *TLR4* changed in the treatments of both AF-MSCs similarly, meaning that it was significantly upregulated by IFNγ (*p*-value = 0.013) and IFNγ (*p*-value = 0.012) cells in the co-culture with T1D PBMCs compared to the HC PBMCs (fig.3-I). Also, the expression level of *TLR4* was almost none by IFNγ cells in the co-culture of HC PBMCs, while it was maximally expressed by IFNγ cells in the T1D PBMCs experiment. Accordingly, the results indicated that

the preconditioning strategy caused a substantial diminish in the *TLR4* level in the MSC/IFNγ during both HC and T1D treatments (*p*-value = 0.0002).

3.4. Molecular analysis of PBMCs

At the end of conditioned medium (CM) and co-culture experiments, the PBMCs were collected and evaluated for the players of immune cell trafficking, including the chemokine ligands *CCL3*, *CCL4*, *CXCL9,* and *CXCL10*, as well as the receptors responsible for pro-inflammatory immune responses, *CXCR3*, *CXCR6*, *CCR5*, and *TLR4*. To minimize the effects of donor variation and attain a consistent assay, the pooled populations of PBMCs were analyzed as representative of each treatment.

3.4.1. Quantitative expression of chemokine ligands in PBMCs

The relative expression of chemokine ligands, *CCL3*, *CCL4*, *CXCL9,* and *CXCL10*, were evaluated in PBMCs at the end of CM culture and co-culture experiments. As depicted by an asterisk in Fig.4-A to -D, the basic culture treatments revealed the only significant difference between HC and T1D PBMCs (the *t*-test *p*-values are 0.012, 0.011, 0.016, 0.020, respectively). These results showed that HC PBMCs expressed all target chemokines at higher levels than that T1D PBMCs in the basic culture treatments. Nonetheless, there were some other differences between HC and T1D PBMCs in which the *p*-values were close to significant levels and depicted in the plots by “ns” (non-significant) marks (fig.4-A to -D). The ANOVA test also displayed remarkable differences and interactions between the expression levels of all target genes among HC and T1D treatments.

In general, the expression of *CCL3* and *CCL4* in HC PBMCs was higher than that in T1D PBMCs across all treatments (*p*-value <0.0001), except for *CCL4* in the treatment of co-cultured with MSC/IFNγ (*p*-value = 0.141). As illustrated in Fig.4-A and -B, *CCL3* and *CCL4* were significantly downregulated in the treatments in which they interacted with MSCs indirectly (cultured in CM) and directly (co-culture experiments) (*p*-value <0.0001), though by stronger effect in HC PBMCs based on their levels in the basic culture treatments. Accordingly, the expression pattern of these genes was rather different between HC and T1D PBMCs, so depending on the preconditioning state two types of cells responded inversely, mostly in co-culture treatments. For example, the interaction analysis by ANOVA displayed that *CCL4* was upregulated by HC PBMCs but downregulated by T1D PBMCs when these cells interacted with IFNγ MSCs compared to the IFNγ MSCs (*p*-value <0.0001). In other words, the expression pattern was inversely altered in two sources of PBMCs based on the preconditioning strategy. It is also worth noting that co-culture versus CM culture did not make any difference in the *CCL4* levels of both PBMCs neither at IFNγ-preconditioned nor non-preconditioned treatments.

Fig.4-C and -D illustrated the expression pattern of *CXCL9* and *CXCL10* which were almost the same across the treatments. However, the genes were inversely expressed in HC and T1D PBMCs based on their preconditioning states. Accordingly, the interaction analysis by ANOVA confirmed a significant relationship between treatments regarding the expression of *CXCL9* (*p*-value = 0.0064) and *CXCL10* (*p*-value = 0.0013). It seems the preconditioning strategy in MSCs differentially affected the expression of

these chemokine ligands in two sources of PBMCs. The CM culture results showed that the CM/IFNγ increased the target genes in HC PBMCs but caused a decrease in T1D PBMCs compared to CM/IFNγ counterparts. Although the results of co-culture treatments revealed no difference in the expression levels in HC PBMCs based on the IFNγ-preconditioning, interaction with the MSC/IFNγ sharply downregulated the genes in T1D PBMCs. Furthermore, the effect of cell contact was rather different between *CXCL9* and *CXCL10*, as well as two sources of PBMCs. In this regard, the IFNγ-preconditioned and non-preconditioned treatments were separately evaluated. The results of IFNγ treatments displayed nearly similar levels of *CXCL9* between CM culture and co-culture in each source of PBMCs, while a similar increasing trend was recorded in both PBMCs due to the co-culture with MSC/IFNγ . Nevertheless, such a comparison in *CXCL10* confirmed a different impact of cell contact in PBMCs, since a decreasing and nearly increasing trend was respectively observed in HC and T1D PBMCs due to their co-culture with MSC/IFNγ , whereas the contact with MSC/IFNγ expressed *CXCL10* at a similar level with the CM culture in HC PBMCs but sharply upregulated that in T1D PBMCs. These observations may also imply the involvement of IFNγ-preconditioning of MSCs in this regard.

3.4.2. Quantitative expression of receptors about immune cell trafficking in PBMCs

The target genes involved in the immune cell trafficking, *CXCR3*, *CXCR6*, *CCR5*, and *TLR4*, were also evaluated in the PBMCs and illustrated in Fig.5-A to -D. The *t*-test analysis concerning the relative expression of *CXCR3* and *CXCR6* revealed non-significant differences between HC and T1D PBMCs in all treatments, however, *CXCR3* was remarkably upregulated in the HC PBMCs cultured in basal medium and T1D PBMCs co-cultured with MSC/IFNγ (*p*-value = 0.054 and 0.129, respectively) compared to their counterparts. Moreover, analysis of *CXCR3* results by ANOVA revealed that the basic culture of both PBMCs (HC and T1D) expressed it at the maximum level, whereas they downregulated it due to indirect (cultured in CM) and direct (co-culture experiments) interactions with MSCs (*p*-value <0.0001) (fig.5-A). The only exception in this case was T1D PBMCs when co-cultured with MSC/IFNγ in which they exhibited *CXCR3* at an almost similar level to the basic culture. The same analysis on *CXCR6* results confirmed the inhibitory effect of MSCs on both sources of PBMCs but only in paracrine conditions where PBMCs were cultured in CM. Nevertheless, this inhibitory effect was not observed in the cell contact situations since *CXCR6* was substantially upregulated (even more than the basic culture) due to the direct interaction of PBMCs with MSCs in the co-culture experiments (*p*-value <0.0001). Hence, both PBMCs (HC and T1D) expressed *CXCR6* at the maximum level in the co-culture with MSC/IFNγ and then with a remarkable drop in the MSC/IFNγ .

As illustrated in fig.5-C, *CCR5* was differentially expressed by two sources of PBMCs, so that the HC PBMCs expressed it more than the T1D PBMCs in the basic culture and culture in the CM/IFNγ (*p*-value = 0.019 and 0.070, respectively), while T1D PBMCs increased *CCR5* at a higher level than that in HC PBMCs during the culture in CM/IFNγ and both co-culture treatments with MSC/IFNγ and /IFNγ (*p*-value = 0.041, 0.344 and 0.064, respectively). Compared to the basic culture, interaction with MSCs upregulated *CCR5* only in HC PBMCs co-cultured with MSC/IFNγ . Still, the gene was augmented in all treatments that the T1D PBMCs were affected by MSCs, particularly in non-preconditioned treatments

(cultured in CM/IFNγ and co-cultured with MSC/IFNγ) (p-value <0.0001). The interaction analysis by ANOVA confirmed a significant relationship between the preconditioning strategy and the cell contact regarding the expression of *CCR5* (p-value = 0.0002). Accordingly, compared to the paracrine conditions, the cell contact in IFNγ treatments led to a moderate decrease of *CCR5* in the HC PBMCs, but a remarkable increase in the T1D PBMCs. On the contrary, the cell contact in IFNγ treatments caused a notable increase in the HC PBMCs, but a fairly decrease in the T1D PBMCs.

The results of *TLR4* (fig.5-D) showed that both PBMCs represent their minimal level in the basic culture where HC PBMCs significantly raised *TLR4* than the T1D PBMCs (p-value = 0.007). Therefore, both sources of PBMCs increased *TLR4* levels due to the interaction with MSCs through the CM and co-culture experiments (p-value = 0.0010). Although the t-test analysis revealed non-significant differences between the two sources of PBMCs in these treatments individually (depicted by the “ns” mark in Fig.5-D), the ANOVA test confirmed the significantly higher level of *TLR4* in the HC PBMCs than the T1D PBMCs among all treatments (p-value = 0.0012). The similar expression pattern of *TLR4* between the two sources of PBMCs suggested a possible same mechanism in these cells affected via the preconditioning strategy, in a way that the IFNγ treatments upregulated the gene in both PBMCs compared to the IFNγ treatments. These findings also imply the lack of the effect of cell contact with MSCs in promoting the expression of *TLR4*.

3.5. A Perspective from the Expression Profile of Target Genes by Heatmaps and Correlation Analysis

The descriptive heatmaps illustrated in Fig.6-A to -D were used to get an overview of the relative expression of target genes between individual treatments. According to the heatmaps representing the levels of the genes in the two treatments of AF-MSCs (MSC/IFNγ and /IFNγ) after the co-culture with the HC PBMCs (Fig.6-A) and the T1D PBMCs (Fig.6-B), obvious discrimination between the two groups is identified. Based on the scale of legends on the right side of the plots, target genes in the MSCs co-cultured with the HC PBMCs display higher expression levels than the cells in co-culture with the T1D PBMCs. However, the expression pattern is highly distinctive between MSC/IFNγ and /IFNγ of each group. For example, the anti-inflammatory genes (*IDO1*, *IDO2*, and *ICAM-1*) were severely enhanced in the MSC/IFNγ compared to the MSC/IFNγ when they were co-cultured with the HC PBMCs, while these genes moderately responded to the interaction with the T1D PBMCs between MSC/IFNγ and /IFNγ . This trend inversely changed regarding the expression of chemokine ligands (*CCL3*, *CXCL9*, and *CXCL10*), so that they softly responded to the interaction with the HC PBMCs in the two treatments, whereas they were remarkably increased in the MSC/IFNγ compared to the MSC/IFNγ due to co-culture with the T1D PBMCs.

The expressional profile of target genes is also depicted by heatmaps for HC PBMCs (Fig.6-C) and T1D PBMCs (Fig.6-D), which are visibly distinctive in the two sources of PBMCs. Based on the scale of legends on the right side of the plots, the HC PBMCs expressed the target genes at higher levels than the T1D PBMCs. However, these genes display obvious discrimination between different treatments of each group based on their expression levels relative to each other. Regarding the expression levels in the basic

culture, the chemokine ligands (*CCL3*, *CCL4*, *CXCL9*, and *CXCL10*) were upregulated in parallel by the T1D PBMCs through co-culture with MSC/IFNγ compared to their counterpart in the HC PBMCs. Furthermore, the inverse pattern of *CCL3* and *CCL4* expression between HC and T1D PBMCs, depending on the preconditioning strategy, are visibly represented in Fig.6-C and -D. Hence, the HC PBMCs enhanced these genes in the IFNγ treatments, whereas T1D PBMCs did it in IFNγ ones. The differences are most apparent in the expression of chemokine receptors *CXCR3*, *CXCR6*, and *CCR5* since, unlike the HC PBMCs, these genes were strikingly upregulated by the interaction of T1D PBMCs with MSCs.

The Pearson correlation analysis was performed after first computing the mean value of replicates concerning the relative expression of target genes among individual treatments and then analyzing those means. The results of correlation analysis in the HC and T1D PBMCs are depicted by the heatmaps Fig.6-E and -F, respectively. Accordingly, Pearson's coefficient of "0.9 to 1" represents positive correlations, and the values of "-0.9 to -1" are indicated as negative correlations, if they are within the significant range (*p*-values < 0.05). The results show interesting differences between the two sources of PBMCs despite the same correlations in them. In this regard, there are the same positive correlations in both PBMC groups, including between *CCL3* and *CCL4* with each other (Pearson's coefficient = 0.99 in HC PBMCs and 0.96 in T1D PBMCs) and altogether with *CXCR3* (Pearson's coefficient ≈1 in HC PBMCs and 0.98 in T1D PBMCs). The most striking difference between the two groups is the positive correlation between *CXCL9* and *CXCL10* which is only evident in the T1D PBMCs (Pearson's coefficient = 0.98). Moreover, there is a possibly negative correlation between *CCL4* and *TLR4* (Pearson's coefficient = -0.91) in the HC PBMCs, as well as a possibly positive correlation between *CCR5* and *TLR4* (Pearson's coefficient = 0.90) in the T1D PBMCs.

3.6. Flow cytometry analysis of T regulatory cells

The pooled PBMCs from individual treatments were used to evaluate the population of Treg cells (CD4 CD25 FOXP3 T cells). For this purpose, the lymphocyte-sized cells were analyzed by these Treg-specific markers and forward scatter (FSC) and side scatter (SSC) parameters. The results of Treg cell proportions in different treatments of HC and T1D PBMCs are illustrated in Fig.7 (A-E) and Fig.8 (A-E), respectively. Based on the results, the substantial distinctions between the Treg cell percentages of the two groups have been recorded. In T1D samples, there was an increase of more than three times in the basic culture (0.49% in HC vs 1.88% in T1D) and more than two times in the treatments of cultured in CM/IFNγ (0.92% in HC vs 2.46% in T1D) and co-cultured with MSC/IFNγ (1.78% in HC vs 3.95% in T1D). In comparison, the only increase in the proportion of Treg cells in the HC samples was observed in the treatment of co-cultured with MSC/IFNγ (2.93% in HC vs 1.08% in T1D). In addition, interaction with MSCs induced the Treg cells in HC PBMCs compared to the basic culture, though by a higher level in the co-culture treatments. However, the culture of T1D PBMCs in CM/IFNγ and their co-culture with MSC/IFNγ reduced Treg cell proportion compared to its level in the basic culture.

Based on the analysis of all treatments, it is evident that two factors markedly influenced the proportion of Treg cells: IFNγ-preconditioning of MSCs, and cell contact with MSCs. The IFNγ-preconditioning of

MSCs had differing impacts on the proportion of Treg cells in HC and T1D samples, depending on whether it was assessed through CM culture or co-culture experiments. Accordingly, a moderate increase of Treg cells in HC PBMCs and a significant decrease in T1D PBMCs was recorded when they were cultured in CM/IFNγ in comparison with CM/IFNγ . However, the co-culture with MSC/IFNγ decreased substantially Treg cells in HC PBMCs but greatly induced them in T1D PBMCs compared to co-culture with MSC/IFNγ . In other words, cell contact was also a key player in the proportion of Treg cells, so it caused the induction of Treg cells in both IFNγ and IFNγ treatments of HC PBMCs. Despite the same trend in the IFNγ treatments of T1D PBMCs, the cell contact led to a decrease in Treg cells in their IFNγ treatments.

Discussion

The crucial role of IFNγ in the destruction of β-cells in pancreatic islets and the development of insulin-dependent diabetes mellitus has been known for several decades (von Herrath and Oldstone 1997). The capacity of IFNγ to regulate the homing of autoreactive CTLs into islets and antigen presentation on β-cells in the islet inflammatory microenvironment suggests it as a main contributor to driving an autoimmune pathology during T1D (De George et al. 2023). In this context, it has been concluded that the genomic background representing T1D patients and their unaffected relatives causes a heightened baseline innate inflammatory state which consequently makes them respond more vigorously against inflammatory stimuli (Cabrera et al. 2016). Therefore, it can be concluded that the imbalance of IFNγ, whether lacking/defective or excessive secretion in the microenvironment, plays an important role in the pathogenesis of the disease. The *in vitro* findings have elucidated the impact of Phytohemagglutinin (PHA) on PBMCs, particularly $CD4^+$ and $CD8^+$ T cells, to generate a pro-inflammatory microenvironment through releasing Th1 cytokines, mainly IFNγ, in culture medium (Mareschi et al. 2016; Li et al. 2021). The Th1 cytokines secreted by PHA-stimulated PBMCs, particularly IFNγ, can polarize MSCs toward an anti-inflammatory state, a process called MSC-licensing/-priming which is essential to induce their immunomodulatory properties (Kim et al. 2018). The licensed MSCs can reciprocally alter the immunophenotype of various T subsets through their paracrine and cell contact effects (Hoseini, Montazeri, Kalantar, et al. 2020).

The present study aimed to explore the possibly different interaction between human AF-MSCs and HC and T1D PBMCs to provide insight into the role of IFNγ-preconditioning and how paracrine and cell contact approaches contribute to this impact. The genes of interest in our study were chosen based on recent findings that have suggested targeting immune cell trafficking toward chronically inflamed tissues for developing new therapeutic interventions in autoimmune diseases like T1D (Sandor, Jacobelli, and Friedman 2019). At the first part of discussion, we will briefly explore the expression of target genes in the AF-MSCs to explain their responses to the co-cultures with two sources of PBMCs. For this purpose, the results of immunomodulatory markers, *IDO1*, *IDO2*, and *ICAM-1*, showed that MSC/IFNγ treatments unexpectedly upregulated them compared to the MSC/IFNγ ones (Fig.3-A, -B, and -C, respectively). It has been previously acknowledged that human MSCs stimulated by IFNγ or exposed to an inflammatory

microenvironment enhance the expression of immunomodulatory markers (Montesinos et al. 2020; Yu et al. 2019). As PHA-stimulated PBMCs generate a pro-inflammatory microenvironment in culture medium through releasing Th1 cytokines, MSC/IFNγ could be overstimulated in co-cultures as a result of the synergistic effect of IFNγ-preconditioning and Th1 cytokines (released via PBMCs) that brings about negative feedback. Meanwhile, the target genes were expressed at a significantly higher level in the MSC/IFNγ co-cultured with HC PBMCs compared to those co-cultured with T1D PBMCs. This indicates that HC PBMCs remarkably induce *IDO1*, *IDO2*, and *ICAM-1* in MSC/IFNγ as the indicators of immunosuppressive capacity, while co-culture with the T1D PBMCs did not achieve the same outcome. This could be related to unknown issues with the downstream pathways of IFNγ in the T1D PBMCs.

It has been identified that MSCs isolated from different tissues can express chemokine receptors and their ligands which play a role in tissue regeneration and immunomodulation, for instance, leukocyte recruitment to inflamed tissues and T cell inhibition potential (Cuesta-Gomez, Graham, and Campbell 2021). Moreover, the cell contact and the IFNγ-preconditioning are both engaged with these mechanisms through modifying a wide range of chemokines and their receptors, such as CXCR3, CXCR6, CCL3, CXCL9, and CXCL10 (Carrero et al. 2012; Kim et al. 2018). Accordingly, our findings have shown that MSCs differently respond to direct contact with HC and T1D PBMCs, which is particularly reflected through the expression of *CCL3* in MSC/IFNγ and *CXCL9* and *CXCL10* in MSC/IFNγ (Fig.3-D, -E and -F, respectively).

The lack of expression of *CCL3* in MSC/IFNγ co-cultured with T1D PBMCs may be due to the production and function of these auAbs in the microenvironment of the experiments. However, the comparable levels of *CCL3* expression in the interactions of MSC/IFNγ with both PBMCs suggest that IFNγ may play a role in triggering this absence in MSC/IFNγ co-cultured with T1D PBMCs. The upregulation of CXCR3 and its ligands (e.g., *CXCL9* and *CXCL10* studied here) on the resident cells of inflamed tissue and infiltrating T cells in response to IFNγ stimulation, suggests a central role for CXCR3-dependent recruitment of immune cells in the pathology of chronic inflammatory diseases (e.g., T1D) and allograft rejection in human and animal models (Hancock et al. 2003; Fallahi et al. 2016). Our findings revealed lower expression of *CXCL9* and *CXCL10* in MSC/IFNγ than that in MSC/IFNγ possibly due to their overstimulation. Additionally, it was interestingly noticed that the levels of *CXCL9* and *CXCL10* expression in MSC/IFNγ displayed an opposite trend when co-cultured with the two sources of PBMCs. Some reports have previously discussed the contrast between the expression of *CXCL9* and *CXCL10*. For example, it has been stated that CXCL10 is expressed more strongly than CXCL9 by pancreatic β-cells after being infected by lymphocytic choriomeningitis virus (Christen et al. 2003). We also observed such an opposite expression pattern in response to IFNγ stimulation in the expression of *CXCR3* and *CXCR6*. Our results showed that co-culturing MSC/IFNγ with HC PBMCs increased CXCR3 but decreased CXCR6 while co-culturing with T1D PBMCs had the opposite effect. In contrast, MSC/IFNγ responded differently in contact with the two sources of PBMCs (Fig.3-G, and -H).

Various types of Toll-like receptors (TLRs) are involved in the polarization of tissue-resident MSCs toward pro-inflammatory or anti-inflammatory phenotypes, a characteristic known as immunoplasticity, which is

a matter of concern in cell therapy approaches. Among them, TLR4 has been described as a trigger of pro-inflammatory phenotype in MSCs (Kurte et al. 2020). Consistent with previous reports, our results confirmed the downregulation of *TLR4* in IFNγ-preconditioned MSCs compared to the MSC/IFNγ (Fig.3-I). Despite the possibility of a heightened anti-inflammatory phenotype in the MSC/IFNγ due to *TLR4* decrease, our investigation into the expression of immunomodulatory markers (*IDO1*, *IDO2*, and *ICAM-1*) did not support this hypothesis. Nonetheless, the significant differences in *TLR4* expression between the two sources of PBMCs can better explain the results of immunomodulatory markers. Given that the pro-inflammatory microenvironment of pancreatic islets is potentially aggressive for the immunosuppressive activity of MSCs (Boland et al. 2018), the increase of *TLR4* in both MSC/IFNγ and MSC/IFNγ as a result of co-culture with T1D PBMCs compared to HC PBMCs, may imply that the microenvironment established by T1D PBMCs is more pro-inflammatory.

To understand more the impact of MSCs on the two sources of PBMCs, we delve deeper into the expression of target genes in the PBMCs at the second part of discussion. Most studies concerning immune cell trafficking to the pancreatic islets have focused on the role of chemokines, e.g. CCL3, CCL4, CXCL9, and CXCL10, and their receptors, including CXCR3, CXCR6, and CCR5 (Sandor, Jacobelli, and Friedman 2019). The chemokine/receptor blockade has been used in intervention studies on animal models that all concluded the association of blocking strategies on these targets with the alleviation and even partial prevention of T1D onset (Carvalho-Pinto et al. 2004; Christen et al. 2003; Morimoto et al. 2004; Sandor et al. 2019). Autoantibodies against CCL3 have been postulated as biomarkers of T1D development owing to higher levels of CCL3 in the serum of patients (Rojewska et al. 2018). Contrariwise, CCL4 has been detected at significantly lower levels in T1D patients (Purohit et al. 2015). In addition, CXCR3 and its ligands, CXCL9 and CXCL10, raise in T1D and several chronic inflammatory diseases (Homann 2015). Despite these findings, which have been obtained from uncultured cells, our results showed that the expression of chemokine ligands (*CCL3*, *CCL4*, *CXCL9*, and *CXCL10*) was higher in HC PBMCs than that in T1D PBMCs after 72 hours of basic culture. Therefore, these results may imply possibly defective pathways responsible for stimulating chemokines in the basic culture of T1D PBMCs.

Recent studies have confirmed the favorable effect of MSCs on reducing the expression level of chemokine ligands by monocytes and DCs (Laranjeira et al. 2022). As anticipated, our results showed that HC PBMCs strongly downregulated *CCL3* and *CCL4* in all MSC-interacted treatments (Fig.4-A and -B). However, these treatments caused T1D PBMCs to express them at a comparable level to the basic cultures, except for *CCL4* in interaction with IFNγ MSCs (both CM and co-culture). These findings highlighted the importance of a preconditioning strategy to empower MSCs for downregulating *CCL3* and *CCL4* in T1D PBMCs. Furthermore, correlation analysis illustrated by the heatmaps Fig.6-E and -F revealed that *CCL3* and *CCL4* are positively correlated with each other in both PBMC groups similarly. They also surprisingly disclosed the same positive correlation with *CXCR3* in two sources of PBMCs. Based on the differing induction of CXCR3 ligands (*CXCL9* and *CXCL10*) on HC and T1D PBMCs in response to IFNγ-preconditioning of MSCs in the CM treatments, it is sensible to assume different interactions of each source of PBMCs with MSCs depending on their preconditioning state. Additionally, there is a similar inconsistency in cell contact experiments, so the preconditioning did not affect *CXCL9*

and *CXCL10* expression levels in HC PBMCs but strongly impacted their expressions in T1D PBMCs. It may imply that T1D PBMCs are more sensitive to cell contact with MSCs in which IFNγ seemingly plays a more decisive role in the group with diabetes compared to the healthy one. The outcome of this inconsistency is reflected in the positive correlation between *CXCL9* and *CXCL10* that was only recorded in the T1D PBMCs.

It has been reported that $CD4^+$ cells expressing CXCR3, CXCR6, and CCR5 are lower among person with diabetes (Hedman et al. 2008) which was reflected in our study through the basic culture of T1D. As previously recognized, the presence of MSCs decreases CXCR3 in immune cells by a dose-dependent manner (Benvenuto et al. 2015), hypothetically attributed to the production of antagonistic CXCL9/10/11 isoforms by MSCs (Chinnadurai et al. 2015). Transplanted MSCs have been reported to lose their suppressive effect when CXCR3 and CCR5 in host cells of animal models are blocked (Han et al. 2022). Our results indicated a restrictive effect of paracrine and cell contact approaches on *CXCR3* expression in HC PBMCs, however, this down-regulatory outcome was not seen in the co-culture of T1D PBMCs with MSC/IFNγ (Fig.5-A). Unlike MSC/IFNγ , the direct contact of MSC/IFNγ was not able to reduce *CXCR3* expression in T1D PBMCs. This also suggests the possible cell contact mechanisms leading to increased levels of this gene in the T1D PBMCs co-cultured with MSC/IFNγ . These results confirm our previous conclusion that T1D PBMCs are more sensitive to surface contact. As presented in the results (Fig.5-B), *CXCR6* was downregulated by two sources of PBMCs due to the paracrine effect of MSCs in the CM cultures, whereas it was substantially upregulated through the cell contact with the MSCs compared to the basic culture. Considering the expression of *CXCR3* and *CXCR6* in the PBMCs, our results suggest an intrinsically different response of these genes to direct contact with MSCs, because, unlike *CXCR3*, *CXCR6* expression was highly sensitive to the cell contact. The MSC/IFNγ treatments significantly upregulated the *CCR5* levels in T1D PBMCs, indicating a higher level of responsiveness compared to HC PBMCs which showed only slight changes during different treatments. This suggests a potential therapeutic benefit of IFNγ MSCs to induce lower level of *CCR5* in T1D patients. As one of the key receptors of innate immunity, the TLR4 is associated with the pathogenesis of diabetes and other chronic inflammatory conditions (Szasz et al. 2016). Previous studies have shown that CD4 T cells co-cultured with MSCs upregulate TLR4 (Selleri et al. 2013) which was reflected in our findings. Former studies have disclosed the higher levels of TLR4 in freshly isolated PBMCs from T1D patients (Zhang et al. 2020; Yin et al. 2022). However, our results displayed a decrease in *TLR4* levels of T1D PBMCs compared to HC PBMCs across all treatments. Some unknown mechanisms might be related to this decline during the cultivation process of T1D PBMCs.

The naturally occurring CD4 CD25 FoxP3 regulatory T cells (nTreg/Treg cells) have been known as the crucial players in restraining inflammation in a variety of autoimmune diseases, including T1D. The activity of Treg cells, which are orchestrated by effector T (Teff) cells, is strongly influenced by the local microenvironment through an intricate network of physiological immune homeostasis (Yarkoni et al. 2008) that has been suggested to be impaired in diabetes-prone strains. *In vitro* studies have demonstrated that a single islet-specific autoantigen can prompt the development of Treg cells during

culture expansion. For instance, it has been known that DCs from autoimmune mice can enhance the quantity and regulatory function of Treg cells by presenting the specific antigen (Tarbell et al. 2004). This was reflected in our results from the basic culture, since Treg cell proportion was higher in T1D PBMCs than HC PBMCs. It is interesting to note that there was a difference in the way Treg cells were induced in two different sources of PBMCs, especially when they were treated with IFNγ MSCs and involved cell contact. Accordingly, the percentage of Treg cells increased when HC PBMCs were co-cultured with MSC/IFNγ and T1D PBMCs were co-cultured with MSC/IFNγ . Our findings indicate a potential association between the preconditioning of MSCs and cell contact, which can impact the induction of Treg cells in T1D PBMCs. Specifically, cell contact with MSC/IFNγ led to an increase in Treg induction, while cell contact with MSC/IFNγ resulted in a significant decrease in Treg induction. A recently published study has also highlighted the role of MSCs in developing iTreg cells in a contact-dependent manner. They demonstrated that silencing the surface marker CD80 in MSCs reduced their capacity to induce iTreg cells, particularly the *in vivo* function to promote selective infiltration of iTreg cells into the transplant site (Mittal et al. 2022). Overall, elucidating the exact mechanisms of MSCs in quantitative and qualitative characteristics of Treg cells in favor of controlling the imbalanced immune responses in autoimmune diseases, including in T1D, is of great importance in theorizing future therapeutic approaches.

Conclusion

Current therapeutic strategies against T1D focus on insulin intensification and β-cell mass preservation, though an MSC-based therapeutic approach has been reported in recent clinical trials. Accordingly, the cell therapy approach requires a proper understanding of the behavior of these cells in the microenvironment of inflamed pancreatic islets in T1D patients. Therefore, we hypothesized that using mitotically active MSCs in two preconditioned and non-preconditioned conditions in interaction with unmodified PBMCs from HC and T1D sources could be enlightening to understand their two-way interactions concerning the IFNγ effect as well as paracrine and cell contact influences in this relationship. Previous studies confirm the role of IFNγ to create an inflammatory microenvironment in the islets and consequently upregulating adhesion molecules and chemokines there. However, the effect of IFNγ on other components of the islet microenvironment, especially on tissue-resident MSCs, remains unclear. As for this study, our objective was not to determine the state of cell preconditioning in cell therapy experiments. Rather, we aimed to demonstrate that the microenvironment resulting from the co-culture of MSCs with PBMCs in T1D patients differs from that of healthy individuals. This finding highlights the significance of this subject in future cell therapy approach and suggests that it requires greater attention.

Declarations

Acknowledgments

Authors gratefully acknowledge Mr. Masoud Tajamolian, for his valuable technical assistance in this work.

Funding

This study was funded by Shahid Sadoughi University of Medical Sciences and Health Services within the framework of a project (grant number: 16575) through a collaboration between the Abortion Research Center and the Yazd Diabetes Research Center.

Conflict of Interests

The authors declare that there is no conflict of interest regarding this article's publication and financial issues.

Ethical Approval

All aspects of the study (blood sampling, data collection) were carried out under the ethical standards of the Shahid Sadoughi University of Medical Sciences and Health Services based on the guidelines of “Declaration of Helsinki”. The study was approved by the *Ethical Committee of Medical School*, Shahid Sadoughi University of Medical Sciences and Health Services.

References

1. Benvenuto, F., A. Voci, E. Carminati, F. Gualandi, G. Mancardi, A. Uccelli, and L. Vergani. 2015. 'Human mesenchymal stem cells target adhesion molecules and receptors involved in T cell extravasation', *Stem Cell Res Ther*, 6: 245.
2. Bernardo, Maria Ester, and Willem E Fibbe. 2013. 'Mesenchymal stromal cells: sensors and switchers of inflammation', *Cell Stem Cell*, 13: 392-402.
3. Boland, L., A. J. Burand, A. J. Brown, D. Boyt, V. A. Lira, and J. A. Ankrum. 2018. 'IFN-γ and TNF-α Pre-licensing Protects Mesenchymal Stromal Cells from the Pro-inflammatory Effects of Palmitate', *Mol Ther*, 26: 860-73.
4. Burke, S. J., and J. J. Collier. 2015. 'Transcriptional regulation of chemokine genes: a link to pancreatic islet inflammation?', *Biomolecules*, 5: 1020-34.
5. Cabrera, S. M., Y. G. Chen, W. A. Hagopian, and M. J. Hessner. 2016. 'Blood-based signatures in type 1 diabetes', *Diabetologia*, 59: 414-25.

6. Calderon, B., J. A. Carrero, M. J. Miller, and E. R. Unanue. 2011. 'Entry of diabetogenic T cells into islets induces changes that lead to amplification of the cellular response', *Proc Natl Acad Sci U S A*, 108: 1567-72.
7. Carrero, R., I. Cerrada, E. Lledó, J. Dopazo, F. García-García, M. P. Rubio, C. Trigueros, A. Dorronsoro, A. Ruiz-Sauri, J. A. Montero, and P. Sepúlveda. 2012. 'IL1β induces mesenchymal stem cells migration and leucocyte chemotaxis through NF-κB', *Stem Cell Rev Rep*, 8: 905-16.
8. Carvalho-Pinto, C., M. I. García, L. Gómez, A. Ballesteros, A. Zaballos, J. M. Flores, M. Mellado, J. M. Rodríguez-Frade, D. Balomenos, and A. C. Martínez. 2004. 'Leukocyte attraction through the CCR5 receptor controls progress from insulitis to diabetes in non-obese diabetic mice', *Eur J Immunol*, 34: 548-57.
9. Chinnadurai, Raghavan, Ian B. Copland, Spencer Ng, Marco Garcia, Mahadev Prasad, Dalia Arafat, Greg Gibson, Subra Kugathasan, and Jacques Galipeau. 2015. 'Mesenchymal Stromal Cells Derived From Crohn's Patients Deploy Indoleamine 2,3-dioxygenase-mediated Immune Suppression, Independent of Autophagy', *Molecular Therapy*, 23: 1248-61.
10. Christen, U., D. B. McGavern, A. D. Luster, M. G. von Herrath, and M. B. Oldstone. 2003. 'Among CXCR3 chemokines, IFN-gamma-inducible protein of 10 kDa (CXC chemokine ligand (CXCL) 10) but not monokine induced by IFN-gamma (CXCL9) imprints a pattern for the subsequent development of autoimmune disease', *J Immunol*, 171: 6838-45.
11. Cuesta-Gomez, Nerea, Gerard J. Graham, and John D. M. Campbell. 2021. 'Chemokines and their receptors: predictors of the therapeutic potential of mesenchymal stromal cells', *Journal of translational medicine*, 19: 156.
12. De George, David J., Tingting Ge, Balasubramaniam Krishnamurthy, Thomas W. H. Kay, and Helen E. Thomas. 2023. 'Inflammation versus regulation: how interferon-gamma contributes to type 1 diabetes pathogenesis', *Frontiers in Cell and Developmental Biology*, 11.
13. Fallahi, P., A. Corrado, A. Di Domenicantonio, G. Frenzilli, A. Antonelli, and S. M. Ferrari. 2016. 'CXCR3, CXCR5, CXCR6, and CXCR7 in Diabetes', *Curr Drug Targets*, 17: 515-9.
14. Figliuzzi, M., B. Bonandrini, S. Silvani, and A. Remuzzi. 2014. 'Mesenchymal stem cells help pancreatic islet transplantation to control type 1 diabetes', *World J Stem Cells*, 6: 163-72.
15. Griffith, J. W., C. L. Sokol, and A. D. Luster. 2014. 'Chemokines and chemokine receptors: positioning cells for host defense and immunity', *Annu Rev Immunol*, 32: 659-702.
16. Han, F., C. Y. Wang, L. Yang, S. D. Zhan, M. Zhang, and K. Tian. 2012. 'Contribution of murine bone marrow mesenchymal stem cells to pancreas regeneration after partial pancreatectomy in mice', *Cell Biol Int*, 36: 823-31.
17. Han, Yuyi, Jianxin Yang, Jiankai Fang, Yipeng Zhou, Eleonora Candi, Jihong Wang, Dong Hua, Changshun Shao, and Yufang Shi. 2022. 'The secretion profile of mesenchymal stem cells and potential applications in treating human diseases', *Signal transduction and targeted therapy*, 7: 92.
18. Hancock, W. W., L. Wang, Q. Ye, R. Han, and I. Lee. 2003. 'Chemokines and their receptors as markers of allograft rejection and targets for immunosuppression', *Curr Opin Immunol*, 15: 479-86.

19. Hedman, Martin, Maria Faresjö, Stina Axelsson, Johnny Ludvigsson, and Rosaura Casas. 2008. 'Impaired CD4+ and CD8+ T cell phenotype and reduced chemokine secretion in recent-onset type 1 diabetic children', *Clinical & Experimental Immunology*, 153: 360-68.
20. Homann, D. 2015. 'Back From the Brink: The Uses of Targeting the CXCL10:CXCR3 Axis in Type 1 Diabetes', *Diabetes*, 64: 3990-2.
21. Hoseini, Seyed, M. , Seyed M. Kalantar, Ahmad R. Bahrami, and Maryam M. Matin. 2020. 'Human Amniocytes: a Comprehensive Study on Morphology, Frequency and Growth Properties of Subpopulations from a Single Clone to the Senescence', *Cell and Tissue Biology*, 14: 102-12.
22. Hoseini, Seyed Mehdi, Maryam Moghaddam-Matin, Ahmad Reza Bahrami, Fateme Montazeri, and Seyed Mehdi Kalantar. 2021. 'Human Amniotic Fluid Stem Cells: General Characteristics and Potential Therapeutic Applications', *The Journal of Shahid Sadoughi University of Medical Sciences*, 28: 3252-75.
23. Hoseini, Seyed Mehdi, Fateme Montazeri, Ahmad Reza Bahrami, Seyed Mehdi Kalantar, Saeede Rahmani, Fateme Zarein, and Maryam Moghaddam Matin. 2020. 'Investigating the expression of pluripotency-related genes in human amniotic fluid cells: A semi-quantitative comparison between different subpopulations, from primary to cultured amniocytes', *REPRODUCTIVE BIOLOGY*, 20: 338-47.
24. Hoseini, SM., F. Montazeri, SM. Kalantar, AR. Bahrami, F. Zarein, and M. Moghadam matin. 2020. 'Mesenchymal Stem Cells: Interactions with Immune Cells and Immunosuppressive-Immunomodulatory Properties', *The Scientific Journal of Iranian Blood Transfusion Organization*, 17: 147-69.
25. Hu, Y., L. Liao, Q. Wang, L. Ma, G. Ma, X. Jiang, and R. C. Zhao. 2003. 'Isolation and identification of mesenchymal stem cells from human fetal pancreas', *J Lab Clin Med*, 141: 342-9.
26. Kim, D. S., I. K. Jang, M. W. Lee, Y. J. Ko, D. H. Lee, J. W. Lee, K. W. Sung, H. H. Koo, and K. H. Yoo. 2018. 'Enhanced Immunosuppressive Properties of Human Mesenchymal Stem Cells Primed by Interferon-γ', *EBioMedicine*, 28: 261-73.
27. Kornicka, Katarzyna, Krzysztof Marycz, Krzysztof Andrzej Tomaszewski, Monika Marędziak, and Agnieszka Śmieszek. 2015. 'The effect of age on osteogenic and adipogenic differentiation potential of human adipose derived stromal stem cells (hASCs) and the impact of stress factors in the course of the differentiation process', *Oxidative Medicine and Cellular Longevity*, 2015.
28. Kurte, Mónica, Ana María Vega-Letter, Patricia Luz-Crawford, Farida Djouad, Danièle Noël, Maroun Khoury, and Flavio Carrión. 2020. 'Time-dependent LPS exposure commands MSC immunoplasticity through TLR4 activation leading to opposite therapeutic outcome in EAE', *Stem Cell Research & Therapy*, 11: 416.
29. Laranjeira, Paula, Mónia Pedrosa, Cátia Duarte, Susana Pedreiro, Brígida Antunes, Tânia Ribeiro, Francisco dos Santos, António Martinho, Margarida Fardilha, M. Rosário Domingues, Manuel Abecasis, José António Pereira da Silva, and Artur Paiva. 2022. 'Human Bone Marrow Mesenchymal

Stromal/Stem Cells Regulate the Proinflammatory Response of Monocytes and Myeloid Dendritic Cells from Patients with Rheumatoid Arthritis', *Pharmaceutics*, 14: 404.

30. Le Blanc, Katarina, and Lindsay C. Davies. 2015. 'Mesenchymal stromal cells and the innate immune response', *Immunology letters*, 168: 140-46.
31. Li, Nina, Hoomann Mirzakhani, Alexander Kiefer, Julia Koelle, Tytti Vuorinen, Manfred Rauh, Zuqin Yang, Susanne Krammer, Paraskevi Xepapadaki, Anna Lewandowska-Polak, Heikki Lukkarinen, Nan Zhang, Barbara Stanic, Theodor Zimmermann, Marek L. Kowalski, Tuomas Jartti, Claus Bachert, Mübeccel Akdis, Nikolaos G. Papadopoulos, Benjamin A. Raby, Scott T. Weiss, and Susetta Finotto. 2021. 'Regulated on Activation, Normal T cell Expressed and Secreted (RANTES) drives the resolution of allergic asthma', *iScience*, 24: 103163.
32. Mareschi, K., S. Castiglia, F. Sanavio, D. Rustichelli, M. Muraro, D. Defedele, M. Bergallo, and F. Fagioli. 2016. 'Immunoregulatory effects on T lymphocytes by human mesenchymal stromal cells isolated from bone marrow, amniotic fluid, and placenta', *Exp Hematol*, 44: 138-50.e1.
33. Mittal, S. K., W. Cho, E. Elbasiony, Y. Guan, W. Foulsham, and S. K. Chauhan. 2022. 'Mesenchymal stem cells augment regulatory T cell function via CD80-mediated interactions and promote allograft survival', *Am J Transplant*, 22: 1564-77.
34. Montesinos, J. J., L. López-García, V. A. Cortés-Morales, L. Arriaga-Pizano, R. Valle-Ríos, G. R. Fajardo-Orduña, and M. E. Castro-Manrreza. 2020. 'Human Bone Marrow Mesenchymal Stem/Stromal Cells Exposed to an Inflammatory Environment Increase the Expression of ICAM-1 and Release Microvesicles Enriched in This Adhesive Molecule: Analysis of the Participation of TNF-α and IFN-γ', *J Immunol Res*, 2020: 8839625.
35. Morimoto, J., H. Yoneyama, A. Shimada, T. Shigihara, S. Yamada, Y. Oikawa, K. Matsushima, T. Saruta, and S. Narumi. 2004. 'CXC chemokine ligand 10 neutralization suppresses the occurrence of diabetes in nonobese diabetic mice through enhanced beta cell proliferation without affecting insulitis', *J Immunol*, 173: 7017-24.
36. Purohit, S., A. Sharma, D. Hopkins, L. Steed, B. Bode, S. W. Anderson, J. C. Reed, R. D. Steed, T. Yang, and J. X. She. 2015. 'Large-Scale Discovery and Validation Studies Demonstrate Significant Reductions in Circulating Levels of IL8, IL-1Ra, MCP-1, and MIP-1β in Patients With Type 1 Diabetes', *J Clin Endocrinol Metab*, 100: E1179-87.
37. Rojewska, Ewelina, Magdalena Zychowska, Anna Piotrowska, Grzegorz Kreiner, Irena Nalepa, and Joanna Mika. 2018. 'Involvement of Macrophage Inflammatory Protein-1 Family Members in the Development of Diabetic Neuropathy and Their Contribution to Effectiveness of Morphine', *Frontiers in Immunology*, 9.
38. Sandor, A M, J Jacobelli, and R S Friedman. 2019. 'Immune cell trafficking to the islets during type 1 diabetes', *Clinical and Experimental Immunology*, 198: 314-25.
39. Sandor, Adam M., Robin S. Lindsay, Nathan Dyjack, Jennifer C. Whitesell, Cydney Rios, Brenda J. Bradley, Kathryn Haskins, David V. Serreze, Aron M. Geurts, Yi-Guang Chen, Max A. Seibold, Jordan

Jacobelli, and Rachel S. Friedman. 2019. 'CD11c+ Cells Are Gatekeepers for Lymphocyte Trafficking to Infiltrated Islets During Type 1 Diabetes', *Frontiers in Immunology*, 10.

40. Sarkar, S. A., C. E. Lee, F. Victorino, T. T. Nguyen, J. A. Walters, A. Burrack, J. Eberlein, S. K. Hildemann, and D. Homann. 2012. 'Expression and regulation of chemokines in murine and human type 1 diabetes', *Diabetes*, 61: 436-46.
41. Selleri, S., M. M. Dieng, S. Nicoletti, I. Louis, C. Beausejour, F. Le Deist, and E. Haddad. 2013. 'Cord-blood-derived mesenchymal stromal cells downmodulate CD4+ T-cell activation by inducing IL-10-producing Th1 cells', *Stem Cells Dev*, 22: 1063-75.
42. Suzdaltseva, Y., K. Goryunov, E. Silina, N. Manturova, V. Stupin, and S. L. Kiselev. 2022. 'Equilibrium among Inflammatory Factors Determines Human MSC-Mediated Immunosuppressive Effect', *Cells*, 11.
43. Szasz, Theodora, Camilla F. Wenceslau, Beth Burgess, Kenia P. Nunes, and R. Clinton Webb. 2016. 'Toll-Like Receptor 4 Activation Contributes to Diabetic Bladder Dysfunction in a Murine Model of Type 1 Diabetes', *Diabetes*, 65: 3754-64.
44. Tarbell, K. V., S. Yamazaki, K. Olson, P. Toy, and R. M. Steinman. 2004. 'CD25+ CD4+ T cells, expanded with dendritic cells presenting a single autoantigenic peptide, suppress autoimmune diabetes', *J Exp Med*, 199: 1467-77.
45. Trivanović, Drenka, Jelena Krstić, Ivana Okić Djordjević, Slavko Mojsilović, Juan Francisco Santibanez, Diana Bugarski, and Aleksandra Jauković. 2016. 'The Roles of Mesenchymal Stromal/Stem Cells in Tumor Microenvironment Associated with Inflammation', *Mediators of inflammation*, 2016: 7314016.
46. von Herrath, Matthias G., and Michael B.A. Oldstone. 1997. 'Interferon-γ Is Essential for Destruction of β Cells and Development of Insulin-dependent Diabetes Mellitus', *Journal of Experimental Medicine*, 185: 531-40.
47. Yang, C., M. Wu, M. You, Y. Chen, M. Luo, and Q. Chen. 2021. 'The therapeutic applications of mesenchymal stromal cells from human perinatal tissues in autoimmune diseases', *Stem Cell Res Ther*, 12: 103.
48. Yarkoni, S., A. Kaminitz, Y. Sagiv, I. Yaniv, and N. Askenasy. 2008. 'Involvement of IL-2 in homeostasis of regulatory T cells: the IL-2 cycle', *Bioessays*, 30: 875-88.
49. Yin, Min, Yan Zhang, Juan Huang, Xinyu Li, Haibo Yu, and Xia Li. 2022. 'Identification of monocyte-related transcriptomic signature of peripheral blood mononuclear cells in type 1 diabetes', *Chinese medical journal*, 135: 2608-10.
50. Yin, Y., H. Hao, Y. Cheng, J. Gao, J. Liu, Z. Xie, Q. Zhang, L. Zang, W. Han, and Y. Mu. 2018. 'The homing of human umbilical cord-derived mesenchymal stem cells and the subsequent modulation of macrophage polarization in type 2 diabetic mice', *Int Immunopharmacol*, 60: 235-45.
51. Yu, Yeonsil, Sae Mi Yoo, Hwan Hee Park, Song Yi Baek, Yoon-Jin Kim, Seunghee Lee, Yu Lee Kim, Kwang-Won Seo, and Kyung-Sun Kang. 2019. 'Preconditioning with interleukin-1 beta and interferon-gamma enhances the efficacy of human umbilical cord blood-derived mesenchymal stem cells-

based therapy via enhancing prostaglandin E2 secretion and indoleamine 2,3-dioxygenase activity in dextran sulfate sodium-induced colitis', *Journal of tissue engineering and regenerative medicine*, 13: 1792-804.

52. Zhang, Xiangdong, Huimin Gu, Li Wang, Feng Huang, and Jin Cai. 2020. 'MiR-885-3p is down-regulated in peripheral blood mononuclear cells from T1D patients and regulates the inflammatory response via targeting TLR4/NF-κB signaling', *The Journal of Gene Medicine*, 22: e3145.
53. Zhou, Y., Y. Yamamoto, Z. Xiao, and T. Ochiya. 2019. 'The Immunomodulatory Functions of Mesenchymal Stromal/Stem Cells Mediated via Paracrine Activity', *J Clin Med*, 8.

Table

Table 1) The primers designed for target genes are listed as their sequence, product size, and Tm.

Gene	Primer sequence	Tm (°C)	Product size (bp)
IDO1	F: GGCAAAGGTCATGGAGATGT	58	127
	R: TCCAGTTTGCCAAGACACAG	58	
IDO2	F: CTGGTCCTGAGCTTCCTCAC	59	153
	R: CAGCACCAAGTCTGAGTGGA	59	
ICAM-1	F: TGATGGGCAGTCAACAGCTA	60	106
	R: GGTAAGGTTCTTGCCCACTG	59	
CXCR3	F: CATAGTTCATGCCACCCAGC	59	105
	R: AAGTCTGGGAGGGCGAAAAG	60	
CXCR6	F: CATGAATGGGTGTTTGGCCA	59	148
	R: CTTGCTGGTTGTAGGCCTTG	59	
CCR5	F: CTATGCCTTTGTCGGGGAGA	59	131
	R: TGTAAACTGAGCTTGCTCGC	59	
CCL3	F: CATCACTTGCTGCTGACACG	59	100
	R: TGGCTGCTCGTCTCAAAGTA	59	
CCL4	F: ATGAAGCTCTGCGTGACTGT	59	127
	R: GCTTCCTCGCGGTGTAAGAA	59	
CXCL9	F: CCTTCCTGCGAGAAAATTGA	60	121
	R: TTTGGCTGACCTGTTTCTCC	60	
CXCL10	F: TTCCTGCAAGCCAATTTTGT	60	99
	R: TCTTGATGGCCTTCGATTCT	59	
TLR4	F: ACCTCCCCTTCTCAACCAAG	59	125
	R: TGTCTGGATTTCACACCTGGA	59	
18S rRNA	F: AGAAACGGCTACCACATCCA	59	158
	R: CCCTCCAATGGATCCTCGTT	59	

Abbreviations) Tm: melting temperature; °C: centigrade; bp: base pair; F: forward primer; R: reverse primer;

Figures

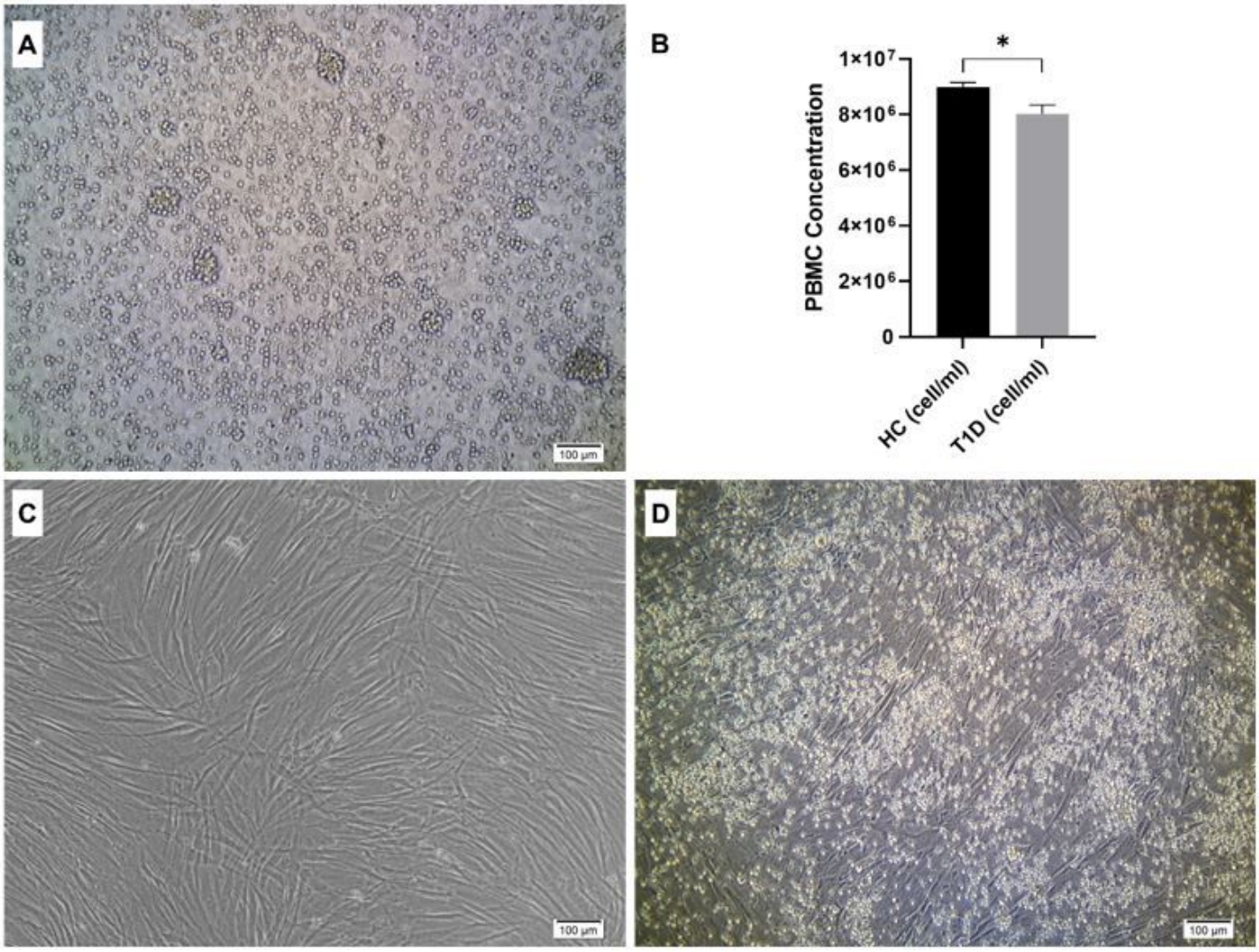

Figure 1

The growth assessment of cultured cells in different situations. **A:** The cultured PBMCs for 48 h by PHA stimulation; **B:** The analysis of PBMC growth by *t*-test as the mean of cell concentration following 48 h culture in healthy control (HC) and T1D groups (p-value < 0.05); **C:** AF-MSCs cultured for 48 h following the third passage as preconditioning phase (with or without IFN-γ). **D**: The direct contact of PBMCs and AF-MSCs in co-culture experiments.

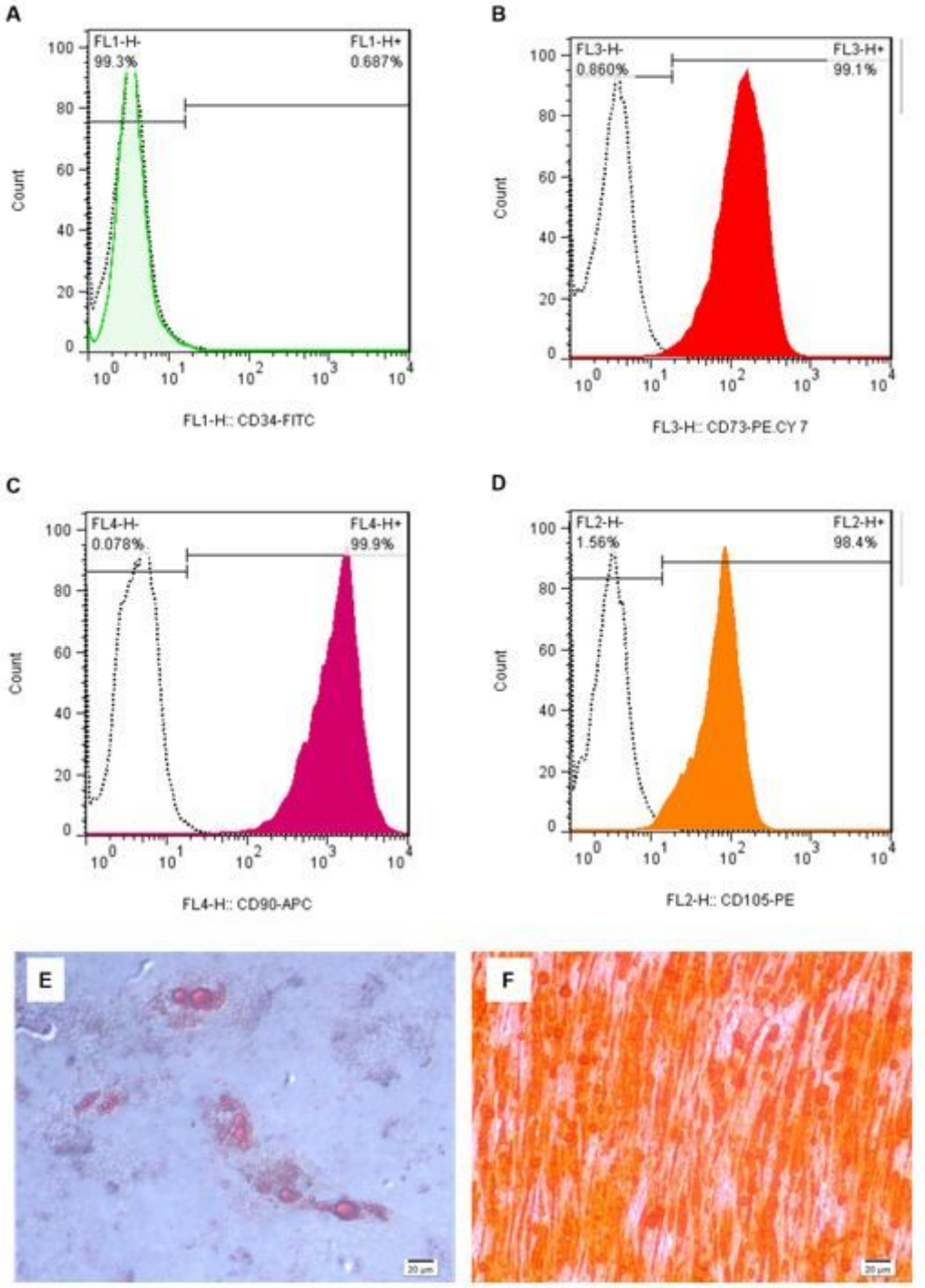

Figure 2

The characterization of AF-MSCs in the 3rd passage. It was performed by flow cytometry analysis (**A**: CD34 as the negative marker; **B**, **C**, **D**: CD73, CD90, CD105, as positive MSC markers, respectively) as well as the mesodermal differentiation (into (**E**) adipocytes and (**F**) osteocytes).

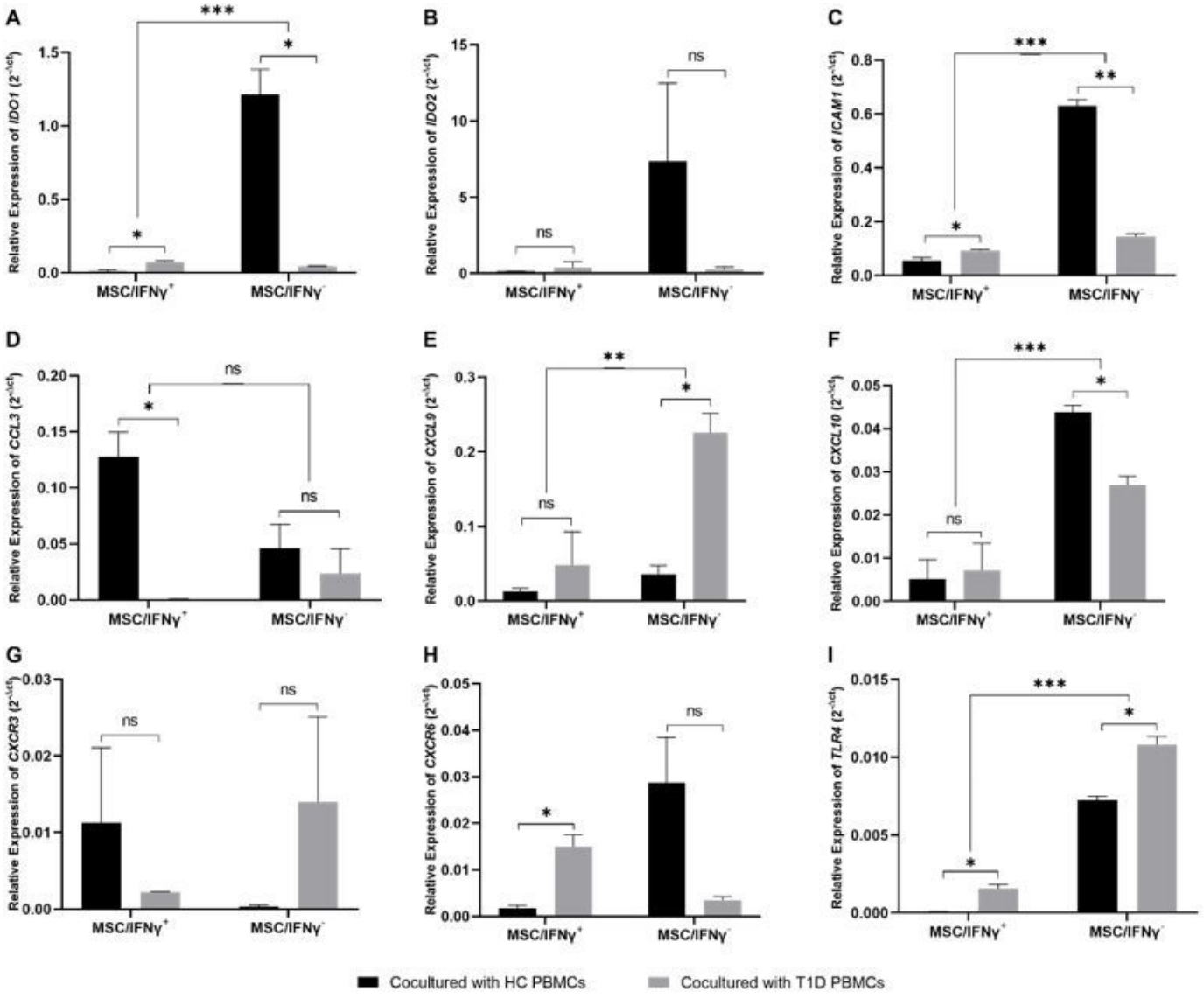

Figure 3

The expression level of target genes in AF-MSCs as IFNγ⁺ and IFNγ⁻ states in co-culture with HC and T1D PBMCs. *IDO1*(**A**), *IDO2* (**B**), *ICAM-1* (**C**), *CCL3* (**D**), *CXCL9* (**E**) and *CXCL10* (**F**), *CXCR3* (**G**), *CXCR6*(**H**) *TLR4* (**I**). The values represent the average of duplicated treatments and standard deviation (SD). The *t*-test was used to analyze the expression levels between AF-MSCs co-cultured with HC and T1D PBMCs. The analysis of variance (ANOVA) test was used to examine the significance of differences among all treatments according to their preconditioning (IFNγ⁺ & IFNγ⁻) and co-culture (HC and T1D PBMCs) conditions. The significant levels are marked as *p*-values non-significant (ns), < 0.05 (*), < 0.01 (**), < 0.001 (***), and < 0.0001 (****).

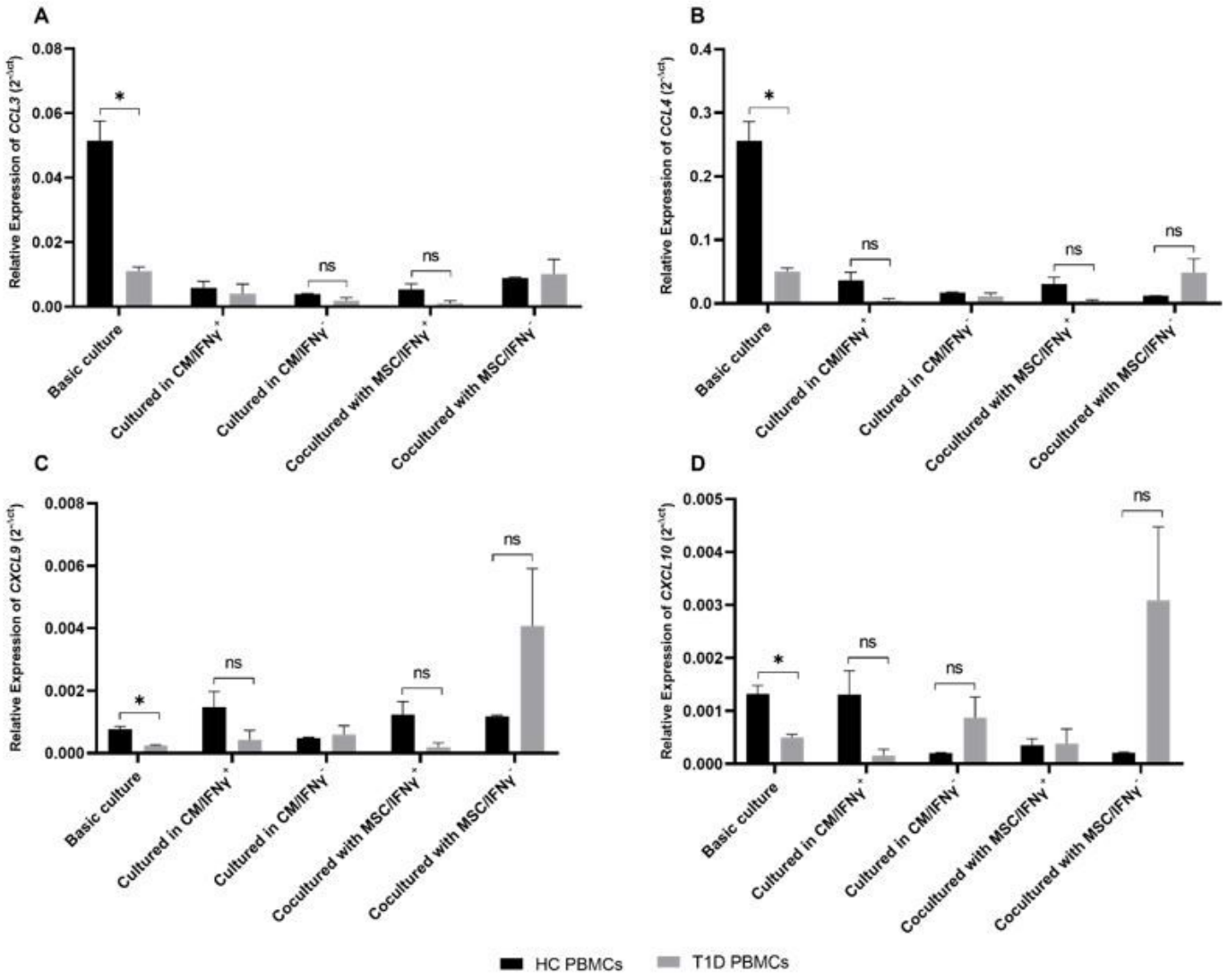

Figure 4

The expression level of chemokine ligands in two sources of HC and T1D PBMCs. The quantitative expression of target genes, *CCL3*(**A**), *CCL4* (**B**) *CXCL9* (**C**), and *CXCL10* (**D**), were evaluated for the average of duplicated treatments as a pooled population of donors and its standard deviation (SD). The treatments are described in the main text. The *t*-test was used to analyze the expression levels between HC and T1D PBMCs in each treatment which their significant levels are marked by asterisks in the plots, as *p*-values non-significant (ns), < 0.05 (*), < 0.01 (**), < 0.001 (***), and < 0.0001 (****). The analysis of variance (ANOVA) test was used to examine the significance among all treatments (*Row Factor p*-values: <0.0001 for A and B; 0.0037 for C; 0.0322 for D) and the possible relationship between treatments (*Interaction p*-values: <0.0001 for A and B; 0.0064 for C; 0.0013 for D). Their significant levels are not marked in the plots.

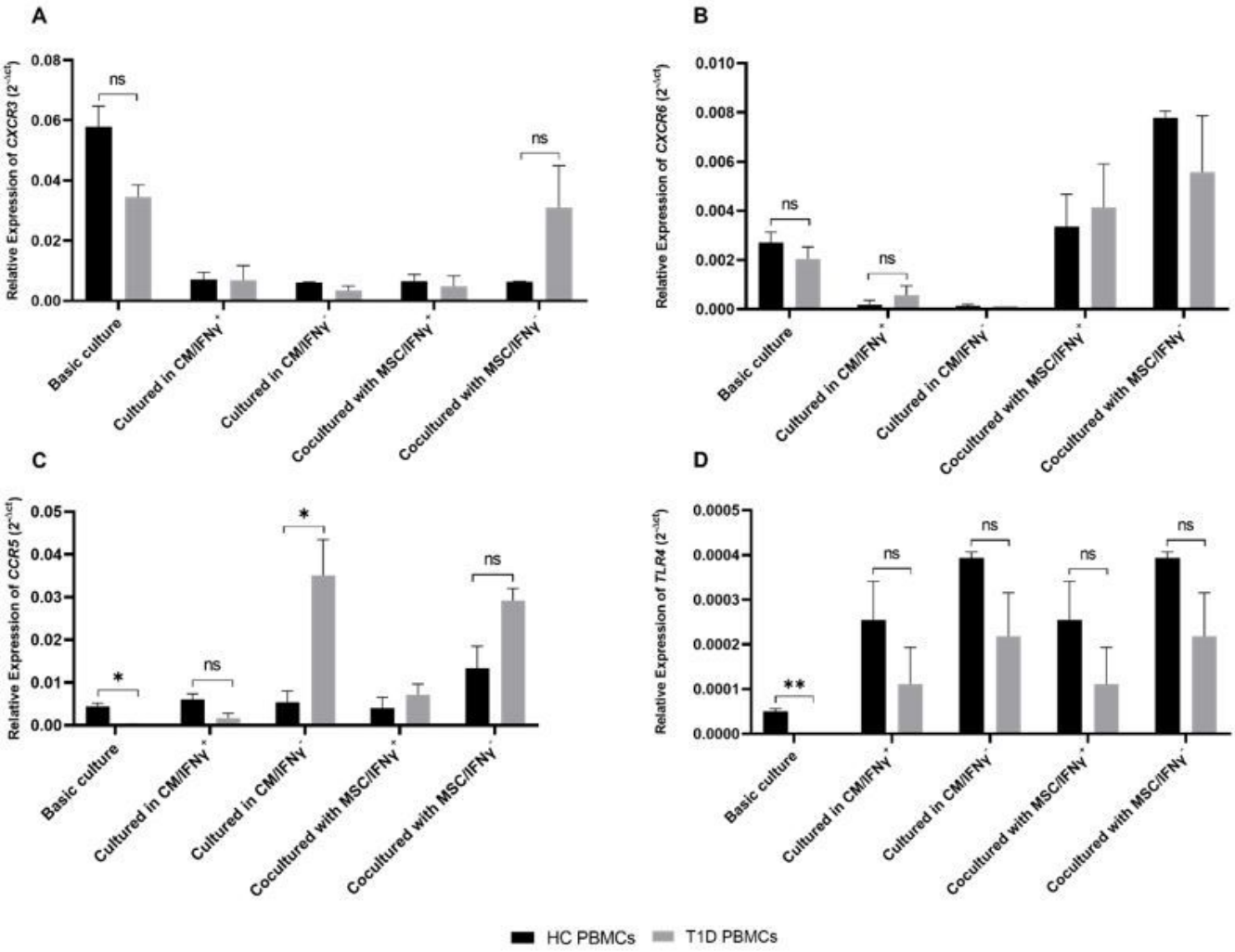

Figure 5

The expression level of receptors about cell trafficking in two sources of HC and T1D PBMCs. The quantitative expression of target genes, *CXCR3*(**A**), *CXCR6* (**B**) *CCR5* (**C**), and *TLR4* (**D**), were evaluated for the average of duplicated treatments as a pooled population of donors and its standard deviation (SD). The treatments are described in the main text. The *t*-test was used to analyze the expression levels between HC and T1D PBMCs in each treatment which their significant levels are marked by asterisks in the plots, as *p*-values non-significant (ns), < 0.05 (*), < 0.01 (**), < 0.001 (***), and < 0.0001 (****). The analysis of variance (ANOVA) test was used to examine the significance among all treatments (*Row Factor p*-values: <0.0001 for A, B, and C; 0.0010 for D) and the possible relationship between treatments (*Interaction p*-values: 0.002 for A; 0.3390 [ns] for B; 0.0002 for C; 0.6980 [ns] for D). Their significant levels are not marked in the plots.

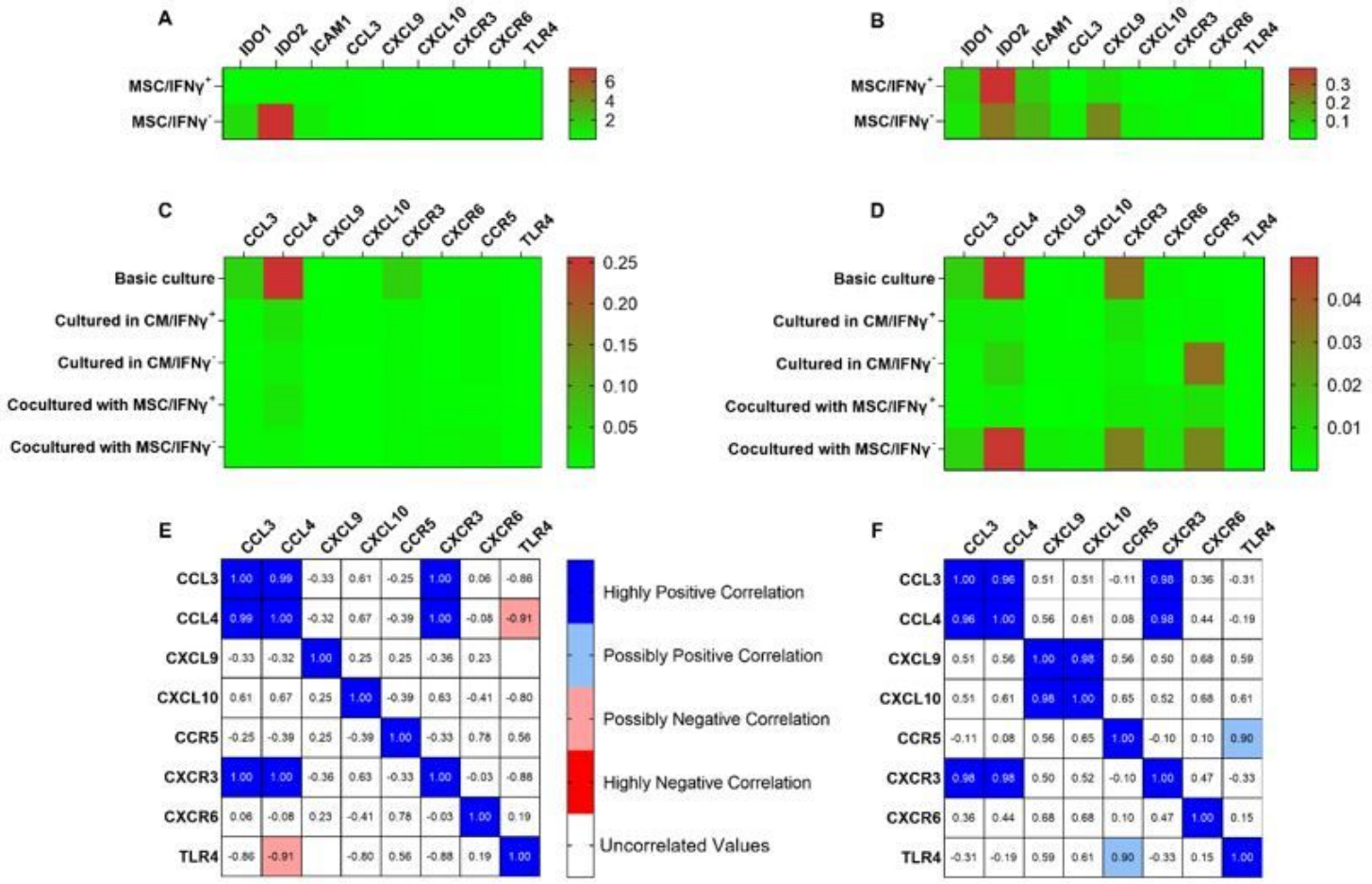

Figure 6

The heatmaps represent the expression level of target genes in different treatments of each cell group and their relationship according to Pearson's coefficient. The expression level of target genes in AF-MSCs co-cultured with HC (**A**) and T1D PBMCs (**B**). The expression level of target genes in HC (**C**) and T1D PBMCs (**D**). The Pearson correlation analysis in HC (**E**) and T1D PBMCs (**F**) (*p*-values < 0.05). The classification of correlations based on Pearson's coefficient: highly positive (0.95 to 1); possibly positive (0.90 to <0.95); possibly negative (>-0.95 to -0.90); highly negative (-1 to -0.95). The non-significant correlations (-0.90< Pearson's coefficient <0.90) are excluded in the heatmaps (white cells).

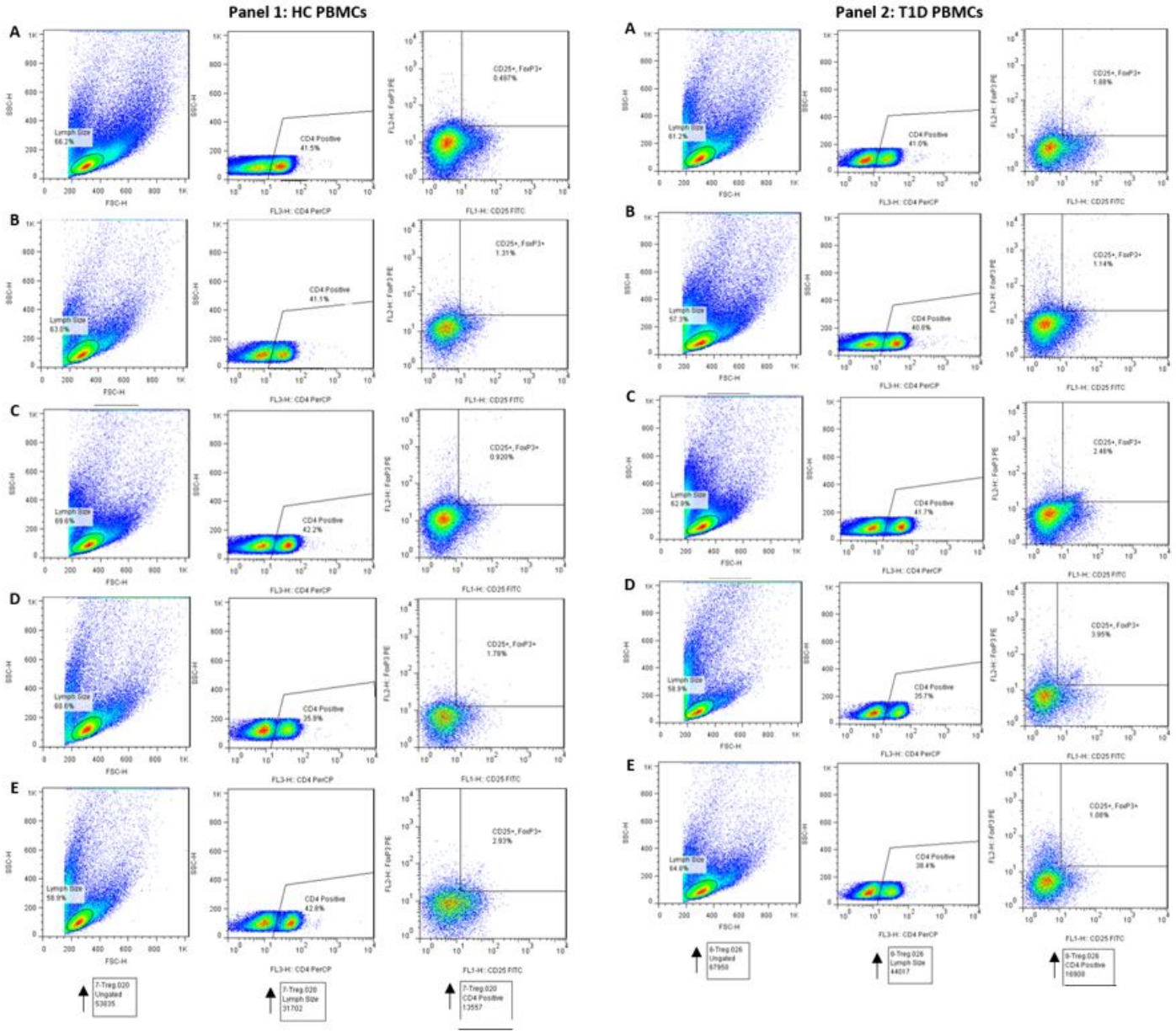

Figure 7

The density dot plots from flow cytometry analysis represent Treg gates. The results are depicted in **Panel 1** for HC PBMCs and **Panel 2** for T1D PBMCs in different treatments: (**A**) Basic culture; (**B**) Cultured in CM/IFNγ ; (**C**) Cultured in CM/IFNγ ; (**D**) Co-cultured with MSC/IFNγ ; (**E**) Co-cultured with MSC/IFNγ . The results of each row depict the order of analysis steps, including the gating based on FSC and SSC parameters to determine lymphocyte-sized cells, the gating of the CD4 population in them, and then the CD25 and FOXP3 population in CD4 cells. **Abbreviations**) FSC: forward scatter; SSC: side scatter.